NACA

RESEARCH MEMORANDUM

TRUE AIRSPEED MEASUREMENT BY IONIZATION-TRACER TECHNIQUE

By Bemrose Boyd, Robert G. Dorsch
and George H. Brodie

Lewis Flight Propulsion Laboratory
Cleveland, Ohio

NATIONAL ADVISORY COMMITTEE
FOR AERONAUTICS

WASHINGTON

July 21, 1952

NATIONAL ADVISORY COMMITTEE FOR AERONAUTICS

RESEARCH MEMORANDUM

TRUE AIRSPEED MEASUREMENT BY IONIZATION-TRACER TECHNIQUE

By Bemrose Boyd, Robert G. Dorsch, and George H. Brodie

SUMMARY

Ion bundles produced in a pulse-excited corona discharge are used as tracers with a radar-like pulse transit-time measuring instrument in order to provide a measurement of airspeed that is independent of all variables except time and distance. The resulting instrumentation need not project into the air stream and, therefore, will not cause any interference in supersonic flow. The instrument was tested at Mach numbers ranging from 0.3 to 3.8. Use of the proper instrumentation and technique results in accuracy of the order of 1 percent.

INTRODUCTION

Tracer techniques have had many applications in aerodynamics research. Various types of tracers including sawdust, smoke particles, regions of heated air, chemical fumes, radioactive molecules, excited molecules emitting afterglow, and ionized molecules have been suggested or used, some quite successfully particularly in the field of flow visualization. Ion bundles or groups of ionized molecules have been found (references 1 to 3) to serve as suitable tracers in the air flow and may be used in conjunction with an accurate timing device in order to provide a fundamental method of measuring airspeed. This method offers definite advantages especially in the region of high supersonic Mach numbers.

Several possible methods for producing the ionization are available including the use of alpha particles, high-speed electrons (either from a resonant cavity as suggested in reference 2, an electron gun, or a radioactive source), ultraviolet rays, X-rays, and various types of electric discharge ranging from a precorona discharge to a spark (references 1 to 3). Work at the NACA Lewis laboratory has indicated that a corona discharge from a needle point mounted in an insulating plug gives better results with respect to the signal produced than a spark discharge and also provides an abundant supply of ions even when the needle point is essentially flush with the surface of the insulator. The selection of ions as tracers and the needle-point corona as ionizing agent permits the instrumentation at both the ionizer and detector to be mounted flush

so as to be outside the air stream, and also permits the use of convenient electronic circuits in both the ionizer supply and the detector amplifier. Three types of operation have been used corresponding to the three types of signal modulation: frequency (reference 2), phase, and pulse-time modulation (references 1 and 3). The selection of the pulse type of operation allows the ionizer supply to be patterned after the high-voltage pulser of a radar transmitter and allows the timer to be patterned after the timing circuit of a radar range unit, thereby providing an accurate direct measurement of pulse transit time for the determination of speed in terms of the fundamental units (time and distance).

The progress that has been made at the Lewis laboratory in the application of a tracer technique to the measurement of true airspeed is outlined herein and an instrument that uses ion bundles or groups of electrically charged molecules for this purpose is described. When measurements between two identical detectors are used, it should be possible to obtain velocity measurements with a high degree of accuracy without inserting any probe into the air stream or otherwise interfering with the flow. Techniques and circuits originating from radar practice and other specialized fields of electronics (references 4 to 7) are combined in this instrument in order to accomplish the specific purpose of accurate airspeed measurement.

The instrument has been tested in six different wind tunnels having cross-section dimensions at the test section ranging from 3.4 inches to 2.0 feet, at Mach numbers ranging from 0.3 to 3.8, and at static pressures from approximately atmospheric down to 0.25 inch of mercury, under conditions of both moist and dry air with temperatures appropriate to the given Mach numbers and pressures. Transit path lengths as short as 1/2 inch have been used.

GENERAL DESCRIPTION OF EQUIPMENT AND METHOD OF OPERATION

The electronic true airspeed indicator measures true airspeed by timing the passage of an ion bundle from one detector to another over a known distance. The instrument is made up of the following components: an ion signal generator consisting of a synchronizer, a high-voltage pulser, and an ionizer electrode; a signal receiver consisting of a detector and an amplifier; a timer; and an oscilloscope indicator. A block diagram (fig. 1) shows the interconnections of the various units in the system. All units operate from the 117-volt, single-phase, 60-cycle power source. Photographs of the instrumentation applied to one of the wind tunnels are presented in figure 2. Figure 3 shows circuit wiring diagrams of the instrument.

The synchronizer (fig. 3(a)) generates two synchronized pulse signals that trigger the driven sweep of the indicator oscilloscope and the high-voltage pulser, respectively. The high-voltage pulser (fig. 3(b)) supplies a pulse (fig. 4) of 7 to 10 microseconds duration and approximately 15,000 volts peak to the ionizer (fig. 5), which is a needle mounted in an insulating insert in the wind tunnel wall so that the point is exposed without protruding into the air stream. The detectors (figs. 5 and 6) are of the induction pickup type also mounted flush in the wind tunnel wall. Two or more detectors may be mounted in line downstream from the ionizer.

An ion bundle is formed in the air stream opposite the ionizer during its period of pulse excitation and is carried downstream by the air flow. A signal (fig. 7) is produced in the receiver by induction when the ion bundle passes each detector. A pulse (fig. 8) also appears in the receiver simultaneously with the ionizer excitation by direct induction from the ionizer. A fixed time delay is incorporated in the pulse channel from the synchronizer to the high-voltage pulser for the purpose of allowing the direct pulse to be viewed on the indicator within the sweep range of the timer.

The timer (fig. 3(d)) is a variable time-delay circuit inserted between the synchronizer and the indicator sweep. The timer enables an operator to position the ion signal from any detector or the direct signal from the ionizer under the indicator index. The crossover or point of zero signal amplitude (fig. 7) provides a measurement point that can be accurately located. The difference between the readings of a calibrated dial on the timer for any two of these signals gives the transit time between the corresponding positions.

DESCRIPTION OF COMPONENTS

Synchronizer. - In the synchronizer unit (fig. 3(a)), a phase-shift master oscillator provides a signal to each of two channels. In each channel the signal is amplified, squared, and peaked to trigger a low-power blocking oscillator. One channel feeds an external synchronizing signal to the timer unit, whereas the other drives a high-power blocking oscillator stage in order to produce the high-voltage-output trigger pulse. This latter signal lags the external synchronizing signal in time phase, and makes it possible to observe on the oscilloscope indicator the pulse that travels to the receiver probe by direct induction as well as the signal resulting from the passage of the tracer ions. Pulse repetition frequencies of 400 and 800 cycles per second have been used.

High-voltage pulser. - The high-voltage pulser (fig. 3(b)) is a commonly used radar pulser circuit. A voltage-doubling rectifier, the amplifier tubes, and the output transformer are connected in series to

produce the high-voltage pulse. The high-voltage pulse transformer is a special unit wound on the powdered-iron core of a television flyback transformer. The transformer is insulated with Teflon and polyethylene tapes and has a voltage step-up of about 1 to 4. The output pulse is bidirectional with a damped oscillatory transient following the negative half cycle (fig. 4). No attempt is made to obtain a unidirectional pulse, as experience has shown that a bidirectional pulse gives better results. The effective width from the first positive half-power point to the trailing negative half-power point is 6 to 8 microseconds. The voltage peaks are of the order of 15,000 volts. When operating under various air pressures it is desirable to control the output of the ion signal generator. This control may be accomplished either by a voltage divider from ionizer to ground or by a variable transformer in the high-voltage supply.

Ionizer. - The ionizer consists of an ionizer electrode and an insulating plug or insert (for example, see fig. 5). The electrode is a needle mounted in the plastic insulator so that the point breaks the surface but does not protrude appreciably. Somewhat better results are obtained when the needle point does project very slightly (less than 0.01 in.) but even in supersonic flow this protrusion usually places the needle point within the subsonic part of the boundary layer. If the ionizer is separately mounted and the voltage does not exceed the voltage necessary to produce the coronal type of discharge, a plug 1 inch in diameter provides adequate insulation except at very low air pressures.

Detector. - The detector (fig. 6) contains the pickup or sensitive element and the input tube, which is a type 9002, connected as a cathode follower. The pickup consists of a shielded wire and insulator assembly in a coaxial configuration ending flush with the inner surface of the wind tunnel wall; the end of the central conductor (No. 14 wire) is exposed to serve as a pickup electrode. The pickup shield diameter is 1/4 inch and its length is 1/2 to 2 inches as required by the tunnel wall thickness. The input grid resistor is 1.5 megohms, which gives a low time constant so that the voltage developed on the input grid is proportional to the induced current rather than to the induced charge.

For use with the interdetector method of measurement (using the transit time and distance from one detector to another) in order to more closely approximate the conditions of measurement at a point, a dual detector has been constructed containing a type 6J6 dual triode with two pickup electrodes mounted just 1/2 inch apart in the same plug and housing, thus providing a transit distance of only 1/2 inch.

Receiver amplifier. - The receiver amplifier (fig. 3(c)) was originally constructed as a video amplifier with a wide pass band and high gain but tests showed that this amplifier was more sensitive than necessary and picked up an excessive amount of noise. The pass band was reduced to about 800 kilocycles and the pentode tubes were reconnected

as triodes in order to handle larger signal amplitudes. The signal from the detector is developed across a 39,000-ohm cathode resistor returned to a negative bias supply in order to extend the dynamic operating range. Two triodes (type 9002) are used in the input in a direct-coupled stage with a high plate load and a low cathode-follower output load resistor. Output to the indicator is taken through capacitive coupling from the cathode of the final stage.

Indicator. - The indicator used in the system is a commercial oscilloscope with provision for a driven (single) sweep with external synchronization. Various types of indication and indexing are possible including circular sweep with radial deflection (J-scope presentation, reference 1), Z-axis blanking or intensification, various forms of electronically generated cursors or time markers, and so forth, but the orthogonal presentation and fixed mechanical index are entirely adequate when used with a delayed and expanded sweep (R-scope presentation).

Timer. - The timing circuit (fig. 3(d)) is a screen-coupled phantastron (reference 4) used in conjunction with appropriate pulse-shaping circuits. The pulse from the synchronizer triggers the phantastron time-delay circuit. After a delay time determined by the control setting, a pulse is produced that triggers the driven sweep in the indicator. Thus the position of any signal with respect to the indicator index is determined by the phantastron control setting in conjunction with the indicator centering control. The time interval between two signals may be obtained by setting first one signal then the other to the index while holding the centering control fixed and noting the difference between the delay times corresponding to the control-dial readings. Calibration of the control dial is accomplished by means of an interval timer connected in such a manner that both the interval timer and the time-delay unit can be started by the same applied pulse, and the timer is stopped by the output pulse from the delay unit. Calibration curves on all ranges show very good linearity and negligible change over periods as long as several months.

BASIS FOR EMPIRICAL DEVELOPMENT OF INSTRUMENT

In spite of a large volume of literature on the general subject of electric discharges in gases (for example, reference 8), no theory was found that adequately covered the production of ion bundles in a moving air stream by a pulsed discharge. Reference 3 contains a theoretical treatment of the signal induced on a pickup electrode by a moving charge which satisfactorily accounts for the shape of the received signal. The current induced in the input circuit (derived in reference 3 and appendix A) may be expressed as

$$i_1 = \frac{q}{V_1} E_2 v \cos \theta$$

where q is the ionic charge, E_2 is the magnitude of the field that would appear at the location of the ion bundle with an assumed arbitrary potential V_1 on the pickup electrode and with the ionic charge absent, and θ is the angle between the field $\overline{E}_2$ and the velocity $\overline{v}$.

Because very little was known about the form of the ionized region produced by a pulsed discharge or its exact location in the air stream, the development of an instrument for using ion bundles in a tracer method of measurement has therefore proceeded on an empirical basis.

Description of signals received. - Two types of received signals have been observed. Both are bidirectional and shaped approximately as would be predicted from the current equation presented previously. One type of received signal which is herein designated type I is first negative-going then positive. (Polarities are given with reference to the input probe. Because there is an odd number of phase reversals in the amplifier, a negative polarity at the amplifier input shows as an upward deflection on the oscilloscope.) The other type of received signal, type II, is first positive-going then negative, and is displaced with respect to the position of the type I signal, the displacement varying with the static pressure of the tunnel atmosphere from 90° advance to almost zero (fig. 9). With either type of signal the crossover or point of zero signal is taken as the measurement point thus making the measurements independent of amplitude fluctuations. Little is known about what causes the appearance of type I and type II signals except that they are evidently produced by regions having net ion charges of opposite sign.

Under the usual conditions of operation, it was found that not every discharge produced an ion bundle of sufficient strength to operate the detector. The proportion of strikes to misses depended on the voltage and current in the discharge and on static pressure in the air stream. The proportion in which the strikes were divided between type I and type II signals also depended on the tunnel air pressure and apparently on the discharge voltage and current (fig. 10).

Experimental observations. - In order to understand the operation of the instrument and to evaluate the interdetector method it has been necessary to consider some data taken with a single detector using the time and distance measured from the ionizer to the detector and also to consider both types of signals. A large number of individual determinations of airspeed have been made and compared, in each case, with the value derived from the best available pressure readings, which usually consisted of total pressure and temperature measured in the tunnel entrance (bellmouth or plenum) and static pressure from wall orifices located near the electronic pickup.

In the tests where the static pressure was varied, it was found that when the ionizer voltage and current were adjusted to give the corona

type of discharge the type I signal was found to be predominant over most of the pressure range and gave reliable results. In one test the shape of the type I signal did vary with pressure as shown in figure 11 but this change did not affect the crossover point and therefore the accuracy of measurement was maintained. This change was apparently not an effect of pressure alone for two reasons: It was not present in tests in other tunnels at higher Mach numbers when the static pressure was as low or lower; and, at least under some conditions, the signal shape could be rectified by adjusting the ionizer voltage. Velocities determined from type II signals with a single detector, on the other hand, underwent a regular shift corresponding to the displacement of the crossover with static pressure. Figure 12 shows the results of a series of measurements using a single detector. In this figure (and elsewhere in this report) the ordinate ϵ is the percentage difference between the velocity measured by the electronic instrument and the velocity determined from pressure readings (see appendix B). At extremely low pressures, both types of signal were attenuated. With the present instrument, the limit of usable signal was between 0.65 and 0.25 inch of mercury corresponding to a pressure altitude between 85,000 and 105,000 feet.

In figure 13 the quantity ϵ is shown as a function of the transit distance D using data obtained with a single detector. A systematic error varying with D is indicated. The single-detector method of operation apparently does not give useful accuracy except possibly when a rather large transit distance is used and either type I signals only are used or the static pressure does not vary.

The use of unsaturated moist air instead of dry air had no effect on the accuracy of velocity measurement. With saturated air the presence of condensation introduced some uncertainty in the comparison of the velocities with those obtained from pressure readings. The intensity of ionization was greater in moist air than in dry air.

RESULTS OF INTERDETECTOR MEASUREMENTS

Either the pressure dependence of the type II signals or the systematic error of the single-detector measurements would preclude the development of a fundamental instrument. Fortunately both of these effects seem to be eliminated by using two detectors and the interdetector transit time and distance. Data obtained by the interdetector method exhibit a random scatter of the values representing individual readings. Figure 14 shows the distribution of values of ϵ for individual interdetector readings. A systematic error of one or two percent is indicated. This error is apparently independent of transit distance.

None of the experimental tests provided any means for determining how much of the difference ϵ should be assigned to the electronic

instrument and how much to the pressure readings. If the nonconstant type of systematic error is, in fact, eliminated by using the interdetector method and if the remaining systematic error in the interdetector readings can be assigned to the pressure instrumentation, as appears reasonable from considerations presented in appendix B, then the electronic instrument can be regarded as a fundamental instrument when two detectors are employed.

There is reason to believe that the random error could be reduced by using electronic means for automatic indexing or for automatic averaging. Any method of averaging, of course, reduces this error in proportion to the number of readings over which the averaging extends. In figure 15, averages of electronic interdetector velocity readings are compared with corresponding averages of velocities obtained from pressure readings. Averages are taken over 50 miles per hour intervals and each point represents from 6 to 22 individual readings for the type I signals and from 4 to 14 readings for the type II signals. The line drawn in this figure has the theoretically correct 45° slope. It can be seen that the agreement of the data is excellent.

DETERMINATION OF EFFECTIVE APPROACH DISTANCE

In any application of the velocity indicator it would be desirable to know the effective approach distance of the ion bundle, that is, the distance between the detector electrode and the nearest point on the trajectory of the effective center of charge. In particular, it is desirable to know how this distance compares with the boundary-layer thickness in any given situation. A possible answer to this question may result from a consideration of the current equation (see appendix A)

$$i_1 = \left(\frac{q}{V_1}\right) \bar{E}_2 \cdot \bar{v} = \left(\frac{q}{V_1}\right) E_2 v \cos \theta$$

The exact nature of the quantity $\bar{E}_2$ depends on the shape of the pickup electrode and its location with respect to any grounded conductors. As a first approximation, the electrode could be assumed to be a point, and located far from any grounded conductors. In this case, the field would be radial with a magnitude $E = \frac{K}{r^2}$, where K is a constant determining the magnitude of the field at unit distance and r is the radial distance from the detector to the ion bundle. A more general condition would be to consider that the actual field in a small element of space in the region of interest around point 2 (point location of ion bundle) could be approximated by a radial field following an inverse power relation, or $E_2 = \frac{K}{r^n}$. If a coordinate system (fig. 16) is chosen with origin

at the pickup electrode, and x-axis parallel to the ion bundle trajectory then $\cos \theta = \frac{x}{r}$ and the approach distance (the perpendicular distance between ion bundle trajectory and pickup electrode) $d = \sqrt{r^2 - x^2}$. When these relations are substituted in the expression for the induced current

$$i_1 = \left(\frac{q}{V_1}\right)\frac{Kvx}{r^{n+1}} = \left(\frac{qKv}{V_1}\right)\frac{x}{(d^2 + x^2)^{\frac{n+1}{2}}}$$

The current peaks will occur when $\frac{di_1}{dx} = 0$, that is, when $\frac{d}{x} = \tan \theta = \pm \sqrt{n}$, or, because $x = vt$,

$$d = \sqrt{n}\, vt_1$$

where t_1 is the measured time interval between the crossover (zero current) point and the peak of the induced current wave form.

In this derivation a point location was assumed for both the ion bundle and the pickup electrode. Data are presented in reference 3 showing that with wide electrodes the peak-to-peak signal width (which, assuming symmetry, is equal to $2t_1$) is a function of electrode width. If asymmetry of the field should cause the current crossover not to coincide with the point of nearest approach of the ion bundle, an error would be introduced in the determination of d. In any practical situation this effect probably would not be large and, moreover, even a knowledge of the order of magnitude of d would be of some value.

A curvature of the field due to nearby grounded conductors would also cause an error through its effect on the directional factor $\cos \theta$. In order to evaluate this error, another hypothetical case is considered. In this case, the electrode has a flat end of negligible dimensions and the field consists of circular arcs as shown in figure 17. Again the magnitude in the region of interest is approximated by $E_2 = \frac{K}{r^n}$, but now $\cos \theta = \frac{x}{s} = \frac{d}{R}$, where R is the radius of the circular line of force passing through point 2. By elementary geometry $\frac{x}{d} = \frac{d}{2R - x}$ or $R = \frac{d^2 + x^2}{2x}$ and $\frac{x}{s} = \frac{d}{R} = \frac{2xd}{d^2 + x^2}$. With the use of this value, the current $i_1 = \left(\frac{2dqKv}{V_1}\right)\frac{x}{(d^2 + x^2)^{\frac{n+2}{2}}}$ and the current maximum occurs when

$$d = \sqrt{n + 1}\ x_1 = \sqrt{n + 1}\ vt_1$$

Thus a correction for the departure of the field from a radial direction based on the rather extreme assumption of circular arcs has the effect of increasing the index by one but leaving the form of the relation between d and x_1 otherwise the same.

Neither of the hypothetical cases studied can completely represent the actual physical situation, but each yields a simple relation for the approach distance d either of which may be expected to give at least the right order of magnitude provided the assumptions regarding geometry and symmetry are satisfied.

Among the data already taken at the Lewis laboratory, only two cases include measurements on both the crossover and peak. For the purpose of calculation it was assumed that the field is radial and $n = 2$ in these two cases, then $d = 0.70$ inch (3.4-in. tunnel at Mach number of 1.5) and $d = 1.03$ inches (1-ft tunnel at a Mach number of 3.2). If $n = 1$, the values of d would be decreased by 30 percent or if $n = 3$ the values would be increased by 22 percent. In the first of these test situations the boundary-layer thickness was probably less than 0.70 inch and the electronic velocity reading was very close to the free-stream value. In the second situation the boundary-layer thickness was probably greater than 1.03 inches and the electronic velocity reading was about 30 percent low. These results are not inconsistent with an interpretation representing ion-tracer formation outside the boundary layer in the first case and within the boundary layer in the second case.

MISCELLANEOUS TESTS AND APPLICATIONS

During tests in the 2- by 20-inch tunnel at low subsonic velocities a signal could be obtained with the detector removed from its mounting and merely held against the outside of the 1/2-inch thick plastic wall of the test section. Also the signal continued when the detector was moved along the wall as far as 30 inches downstream from the ionizer. Such a procedure seems to offer possibilities as a method of flow tracing.

The nature of the pulse system used does not give a continuous indication of air speed but rather a series of instantaneous samples, each representing an average speed over a portion of a streamline. The unsteadiness of the signal in the direction of the time axis, which is mentioned in connection with the random error in appendix B may be observed by eye, or photographically, or measured by noting the timer dial readings at the limits of fluctuation. Insofar as this effect is a result of large scale turbulence, such measurements should give some information about the longitudinal component of the turbulence. An

automatic system using the two-detector method coupled into a start-stop timer circuit could be constructed for recording either instantaneous samples or running averages of consecutive values.

In addition to the primary application, that is, to provide measurement without introducing shock waves in supersonic flow, flush instrumentation may be advantageous in situations where it is desirable to reduce the drag caused by conventional sensing devices or their supports, where instrumentation is adversely affected by high temperatures or erosion, or where its presence may cause increased ice accumulation. Other suggested uses include the possibility of metering the flow of dielectric liquids, missile speed timing, and so forth.

CONCLUDING REMARKS

A consideration of the application of tracer techniques to the measurement of airspeed has led to evaluation of the types of tracer materials, the methods of producing the tracers, and the methods of system operation that yield satisfactory results. An empirical process of development has resulted in an instrument which operates by modulating the state of ionization of the air flow and electronic timing between two similar detectors and gives airspeed directly in terms of time and distance independently of ambient conditions of temperature, pressure, or humidity.

A comparison of the readings of this instrument with airspeed values calculated from pressure readings shows a systematic difference of 1 or 2 percent. If, as seems to be indicated although not proven, this difference represents an error in the pressure readings, the remaining error of the electronic instrument can be made as small as desired by averaging a number of consecutive readings.

A theoretically derived and, as yet, untested method for determining experimentally the effective approach distance or location of the tracer path is presented.

Possible applications to flow tracing and turbulence measurement are discussed.

Lewis Flight Propulsion Laboratory
National Advisory Committee for Aeronautics
Cleveland, Ohio

APPENDIX A

THEORY OF INDUCTION-PICKUP WAVEFORM

Green's reciprocation theorem in electrostatics (reference 9) states that if $V_1, V_2, \ldots V_n$ are the potentials produced on elements of conducting surfaces (or on the separate conductors of a system) 1, 2, . . . n by a distribution of charges $Q_1, Q_2, \ldots Q_n$ and if a different distribution of charges $Q_1', Q_2', \ldots Q_n'$ on the same system of conductors produces potentials $V_1', V_2', \ldots V_n'$, then $\sum_n V_n Q_n' = \sum_n V_n' Q_n$.

In applying this to the velocity-indicator situation, conductor 1 is the pickup electrode and conductor 2 is assumed to be a conductor of infinitesimal dimensions located at the position of the center of the ion bundle. The assumed charge and potential distributions are: (1) The ionic charge is not present, that is $Q_2 = 0$, but an arbitrary potential V_1 (which may be a unit potential) is applied to conductor 1, producing on it a charge $Q_1 = q_1$ and a field E_2 and potential V_2 at point 2; (2) conductor 2 carries the ionic charge (assumed constant) and conductor 1 is grounded so that $Q_2' = q$, $V_1' = 0$, $Q_1' = q_1'$ (unknown) and V_2' equals the potential at point 2 corresponding to the field E_2' at that point which results from the given charge distribution.

Then by Green's theorem:

$$q_1' V_1 + q V_2 = 0$$

$$q_1' = -\frac{q V_2}{V_1}$$

In this equation q and V_1 are constant and V_2 is constant for any given position of point 2 but becomes a function of time when point 2 moves. In accordance with Shockley (reference 10), the current through a conductor connecting conductor 1 to ground is

$$i_1 = \frac{dq_1'}{dt} = -\left(\frac{q}{V_1}\right)\frac{dV_2}{dt}$$

Because V_2 is a function of the coordinates of point 2 $\left(\frac{dV_2}{dt} = \frac{\partial V_2}{\partial x}\frac{dx}{dt} + \frac{\partial V_2}{\partial y}\frac{dy}{dt} + \frac{\partial V_2}{\partial z}\frac{dz}{dt} = \nabla V_2 \cdot \frac{d\bar{r}}{dt}\right)$, the current may be written

$$i_1 = -\left(\frac{q}{V_1}\right)\nabla V_2(r) \cdot \frac{d\bar{r}}{dt} = \left(\frac{q}{V_1}\right)\bar{E}_2 \cdot \bar{v}$$

or

$$i_1 = \left(\frac{q}{V_1}\right) E_2 v \cos\theta$$

where $\bar{r}$ is the position vector of point 2 with respect to point 1 and θ is the angle between the field and velocity vectors.

APPENDIX B

ANALYSIS OF ERRORS

Experimental observations together with an analysis of the error equation

$$\epsilon = \frac{\frac{D+d}{T+t} - (V+v)}{V + v} \times 100$$

where D = transit distance (measured by electronic instrument)

T = transit time (measured by electronic instrument)

V = true airspeed (measured by pressure instruments)

d, t, v = errors in foregoing quantities, respectively

indicate that three types of error cover all of the most probable sources: (1) A constant error in transit time or distance produces a systematic component of ϵ which is a hyperbolic function of D, (2) A constant error in the pressure-determined velocity produces a systematic component of ϵ which is independent of D, and (3) A rapid fluctuation of the signal image on the indicator, which may at least in part be due to turbulence in the air stream, requires a visual averaging which together with other reading errors produces a random component of ϵ.

The curves drawn through the single-detector data points in figure 13 represent the hyperbolic functions $(\epsilon - 0.4)\ D = 21.6$ and $(\epsilon - 0.4)\ D = -32.5$.

REFERENCES

1. Munnikhuysen, R. D.: High Range True Air-Speed Indicator. Air Technical Intelligence, Technical Data Digest, vol. 13, no. 5, Mar. 1, 1948, pp. 7-12.

2. Mullen, Glenn L.: Gas-Flow Speedometer. Electronics, vol. 23, no. 2, Feb. 1950, pp. 80-81.

3. Anon.: Measurement of Gas Velocity by Pulsed Ionization Technique. National Research Corp., May 31, 1951. (Contract N7onr-478.)

4. Chance, Britton, et al., editors: Electronic Time Measurements. McGraw-Hill Book Co., Inc., 1949.

5. Chance, Britton, et al., editors: Waveforms. McGraw-Hill Book Co., Inc., 1949.

6. Valley, George E., Jr., and Wellman, Henry, editors: Vacuum Tube Amplifiers. McGraw-Hill Book Co., Inc., 1948.

7. Ridenour, Louis N., editor: Radar System Engineering. McGraw-Hill Book Co., Inc., 1947.

8. Loeb, Leonard B.: Fundamental Processes of Electrical Discharge in Gases. John Wiley & Sons., Inc., 1939.

9. Jeans, J. H.: The Mathematical Theory of Electricity and Magnetism. Cambridge Univ. Press, 5th ed., 1948, p. 92.

10. Shockley, W.: Currents to Conductors Induced by a Moving Point Charge. Jour. Appl. Phys., vol. 9, no. 10, Oct. 1938, pp. 635-636.

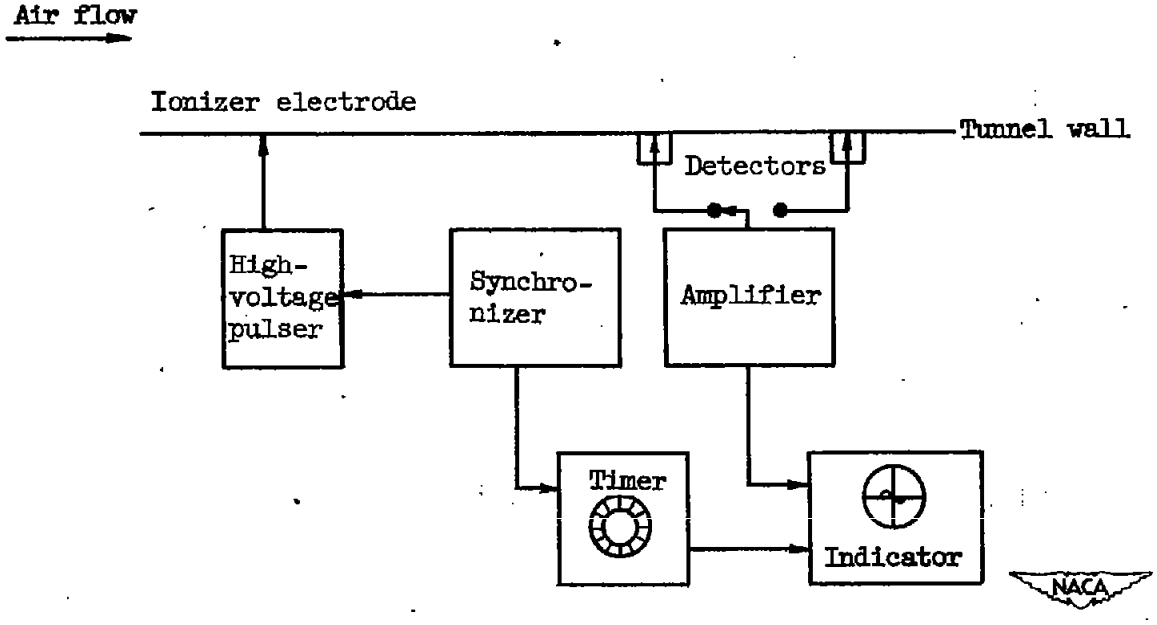

Figure 1. - Block diagram of electronic true airspeed indicator.

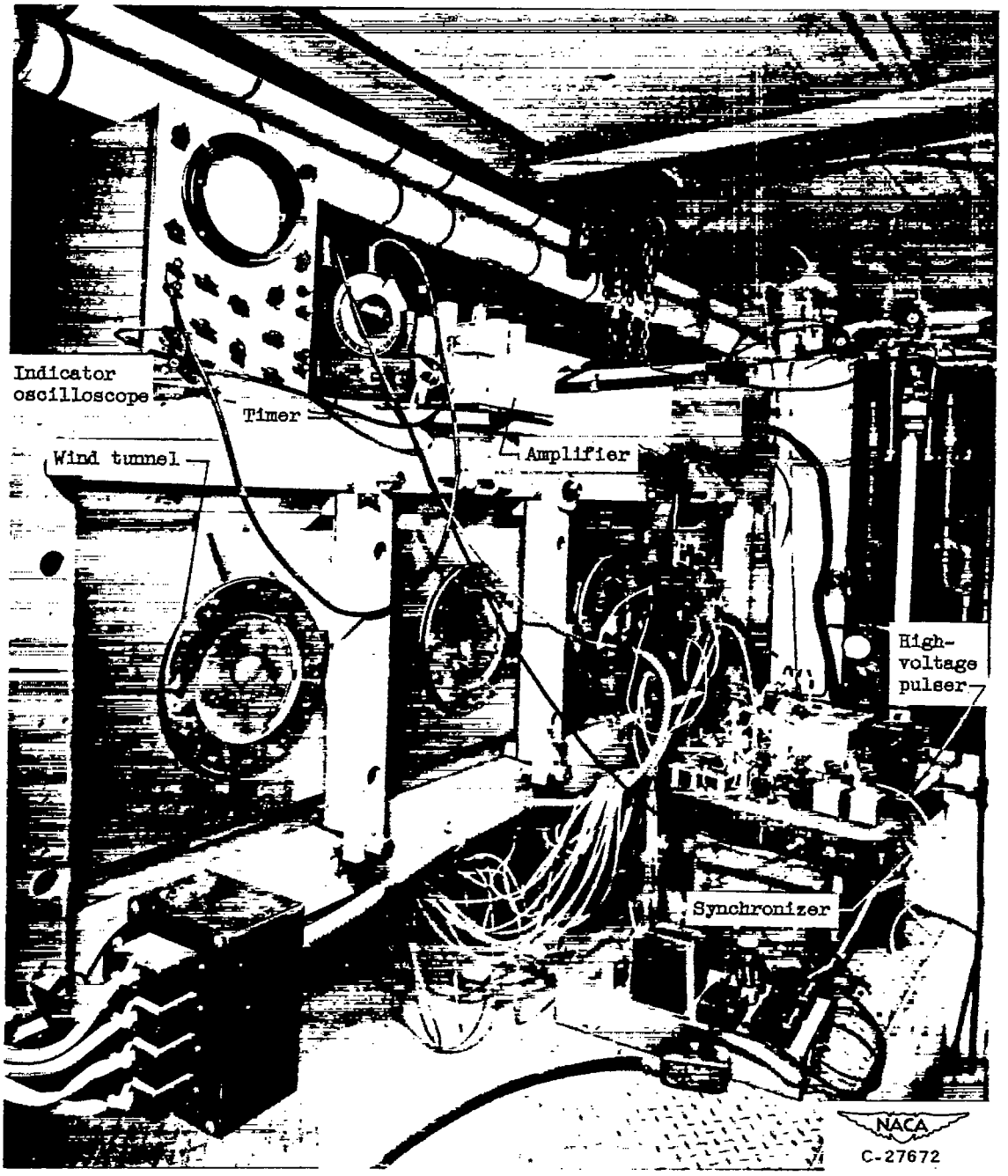

(a) General view.

Figure 2. - Electronic true airspeed indicator in 4- by 10-inch wind tunnel.

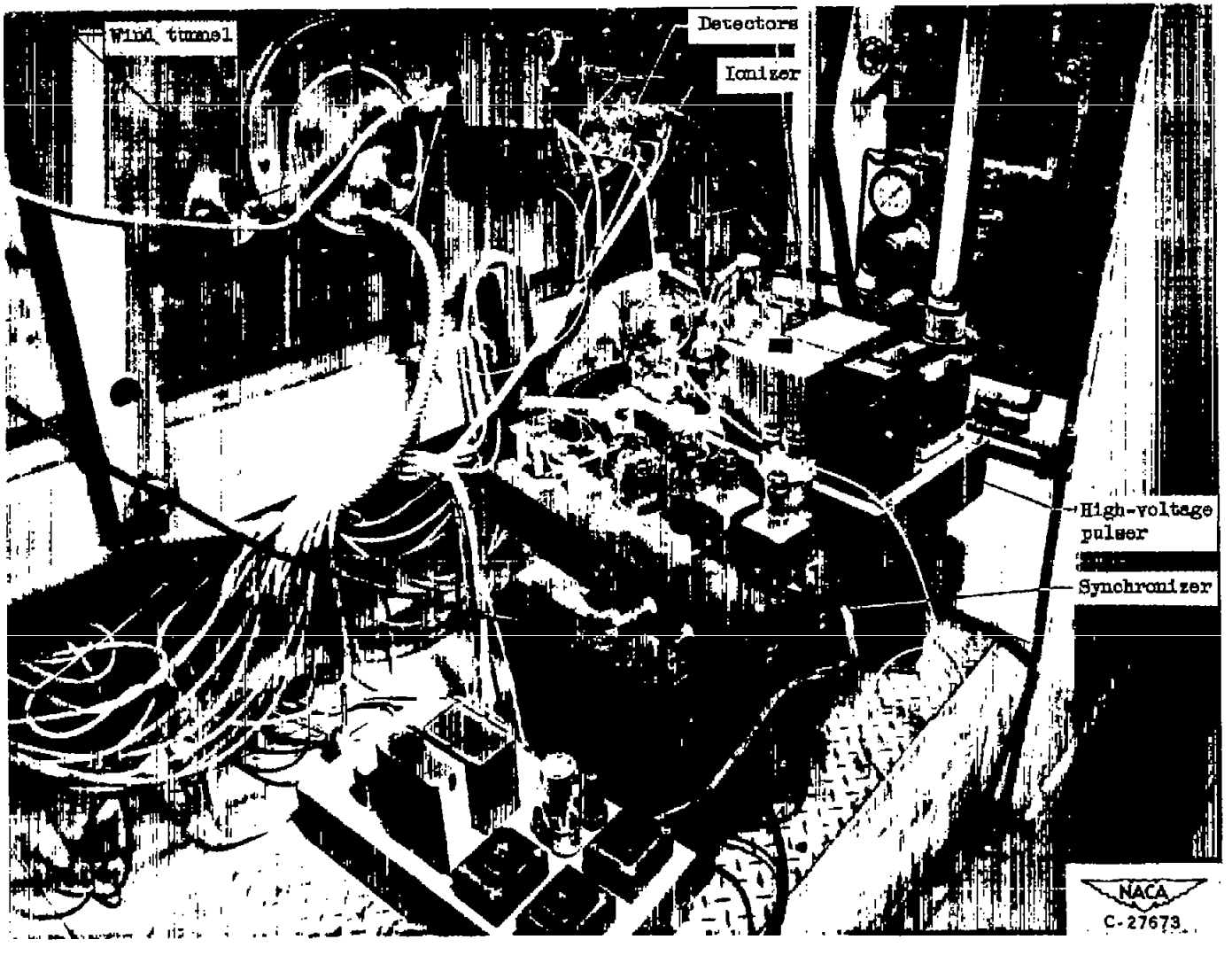

(b) Ion signal generator, ionizer, and detectors.

Figure 2. - Continued. Electronic true airspeed indicator in 4- by 10-inch wind tunnel.

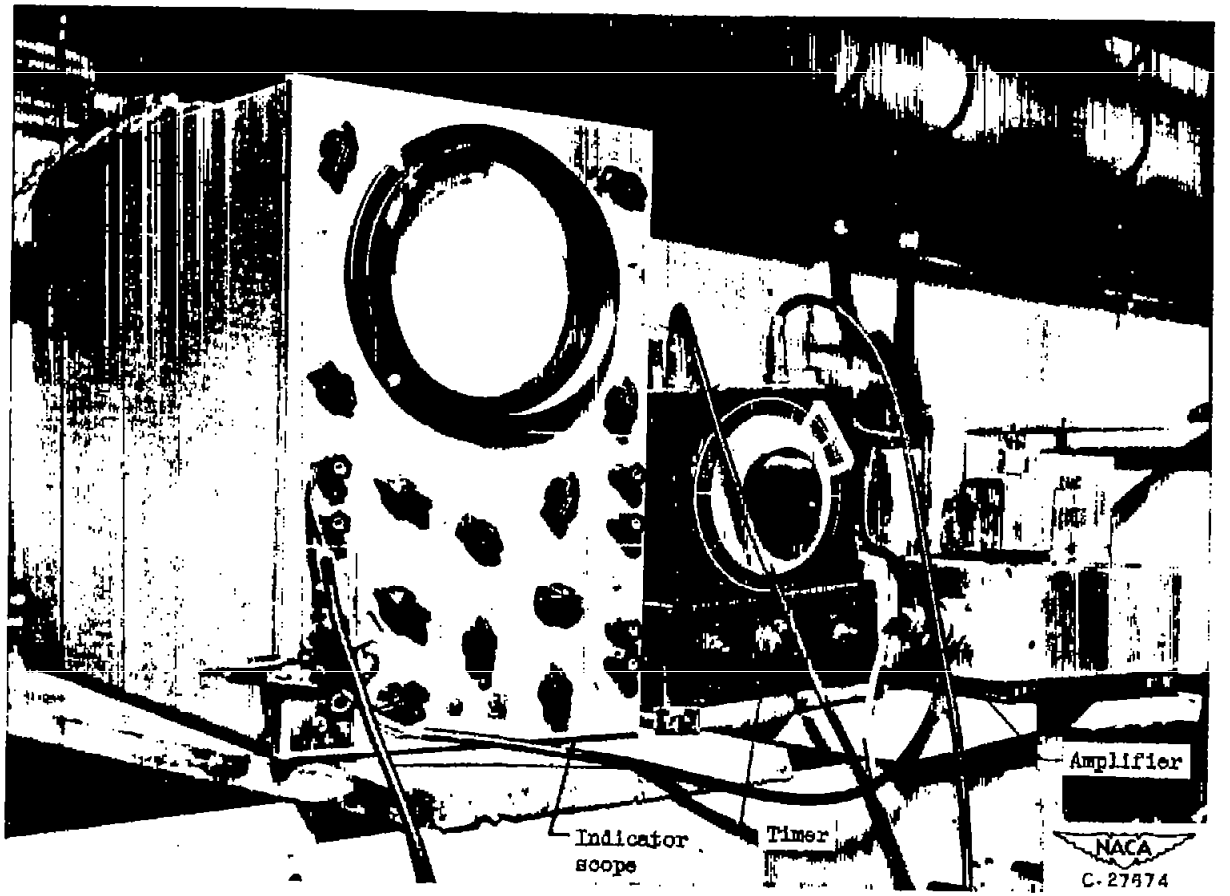

(c) Amplifier, timer, and indicator.

Figure 2. - Concluded. Electronic true airspeed indicator in 4- by 10-inch wind tunnel.

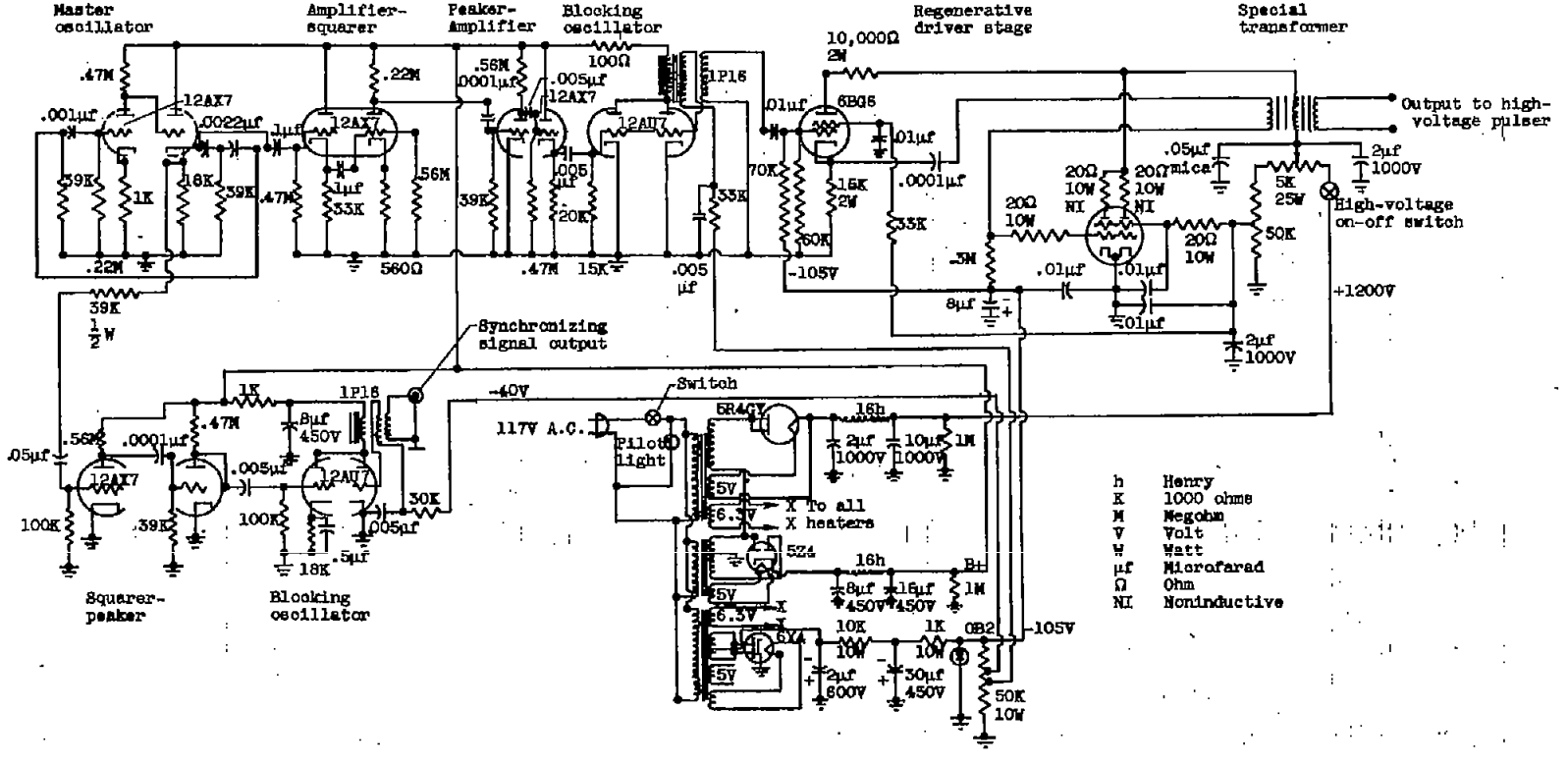

(a) Synchronizer.

Figure 3. - Electronic true airspeed indicator.

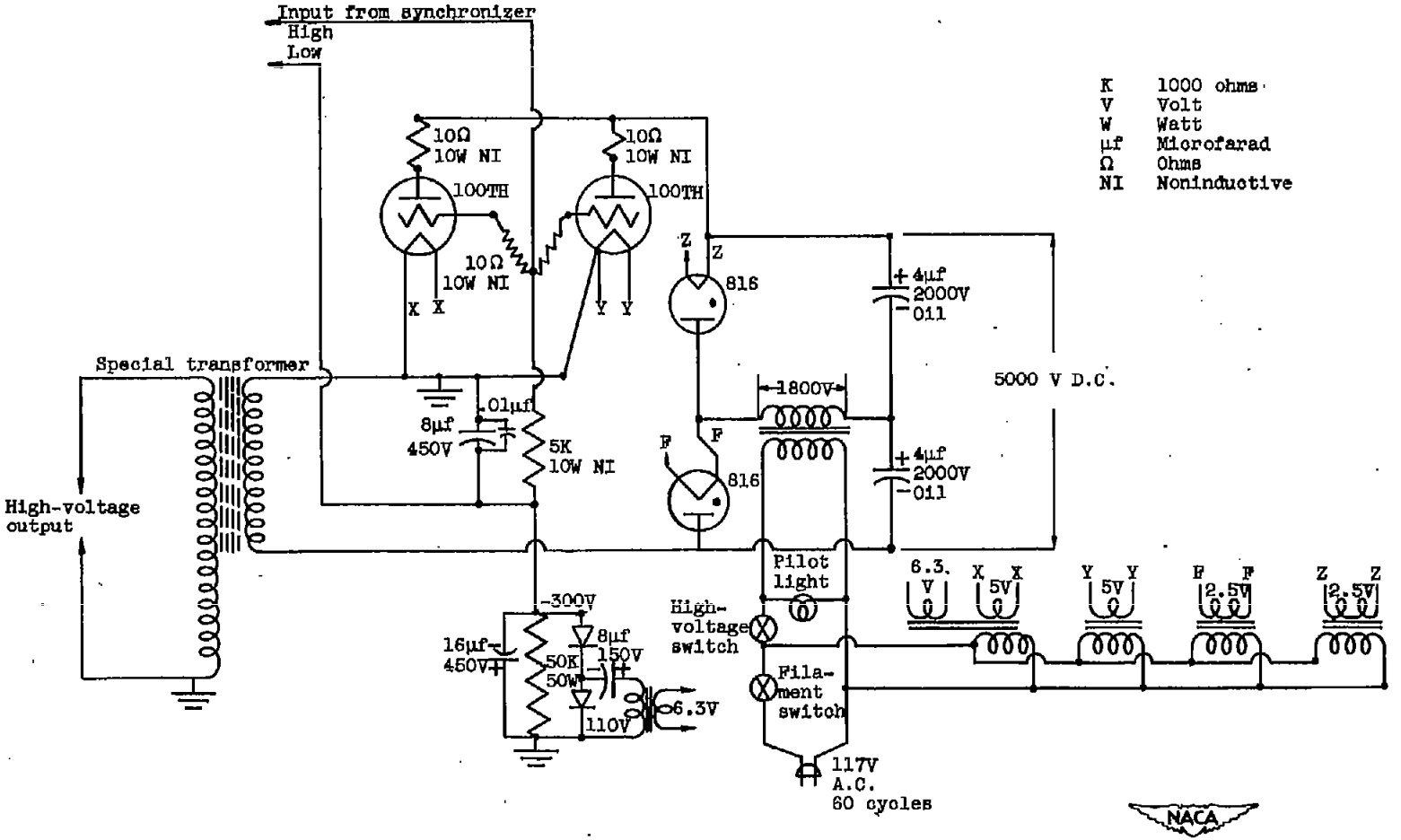

(b) High-voltage pulser.

Figure 3. - Continued. Electronic true airspeed indicator.

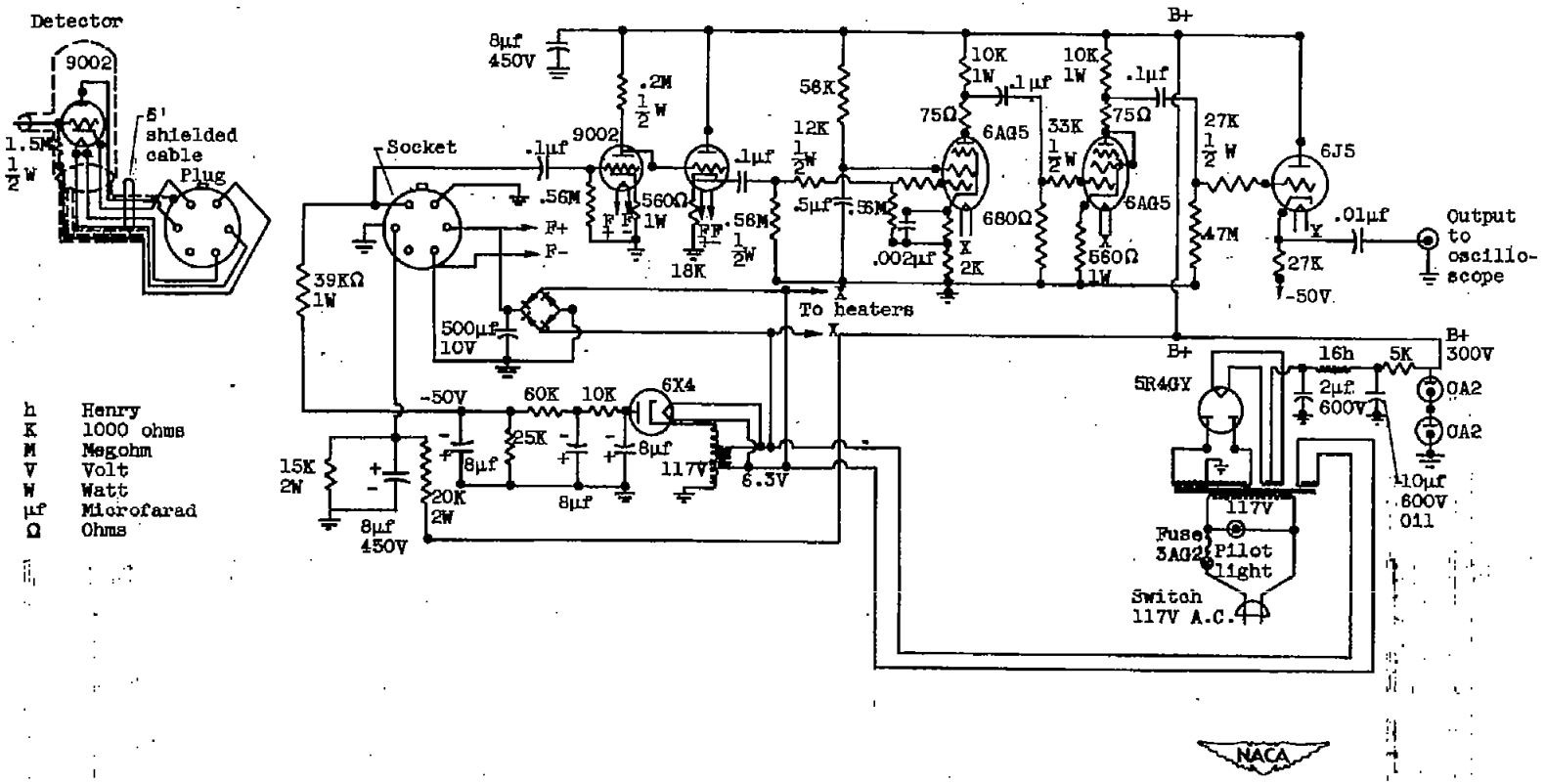

(c) Receiver unit.

Figure 3. - Continued. Electronic true airspeed indicator.

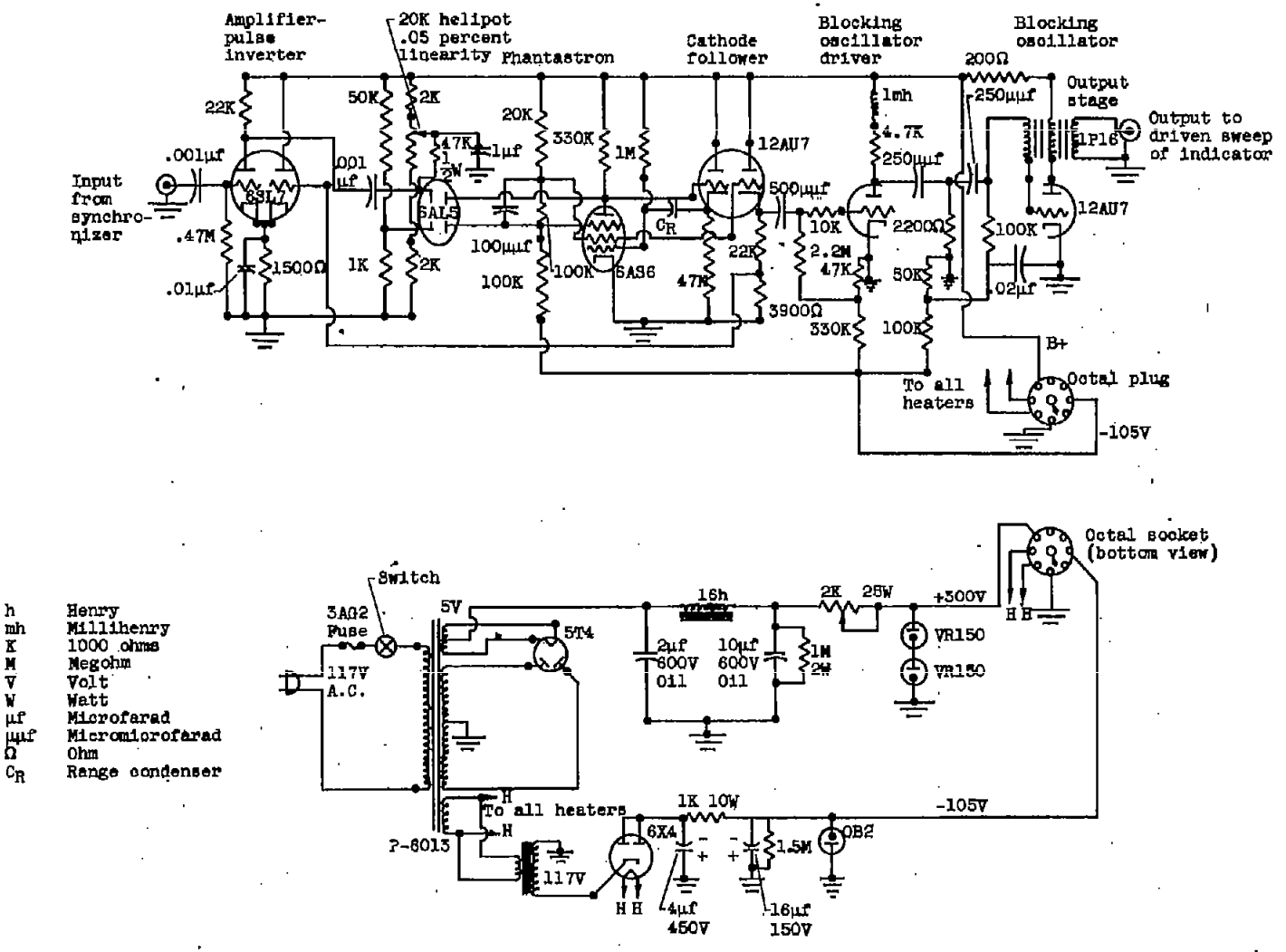

h	Henry
mh	Millihenry
K	1000 ohms
M	Megohm
V	Volt
W	Watt
µf	Microfarad
µµf	Micromicrofarad
Ω	Ohm
C_R	Range condenser

(d) Timer unit.

Figure 5. - Concluded. Electronic true airspeed indicator.

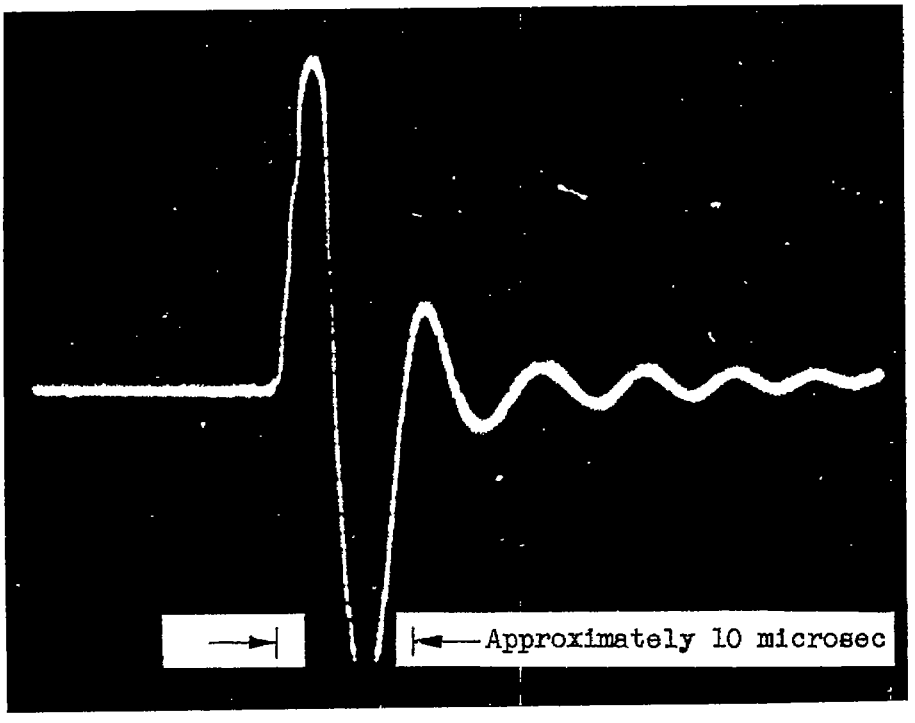

Figure 4. - Wave form of pulse applied to ionizing needle.

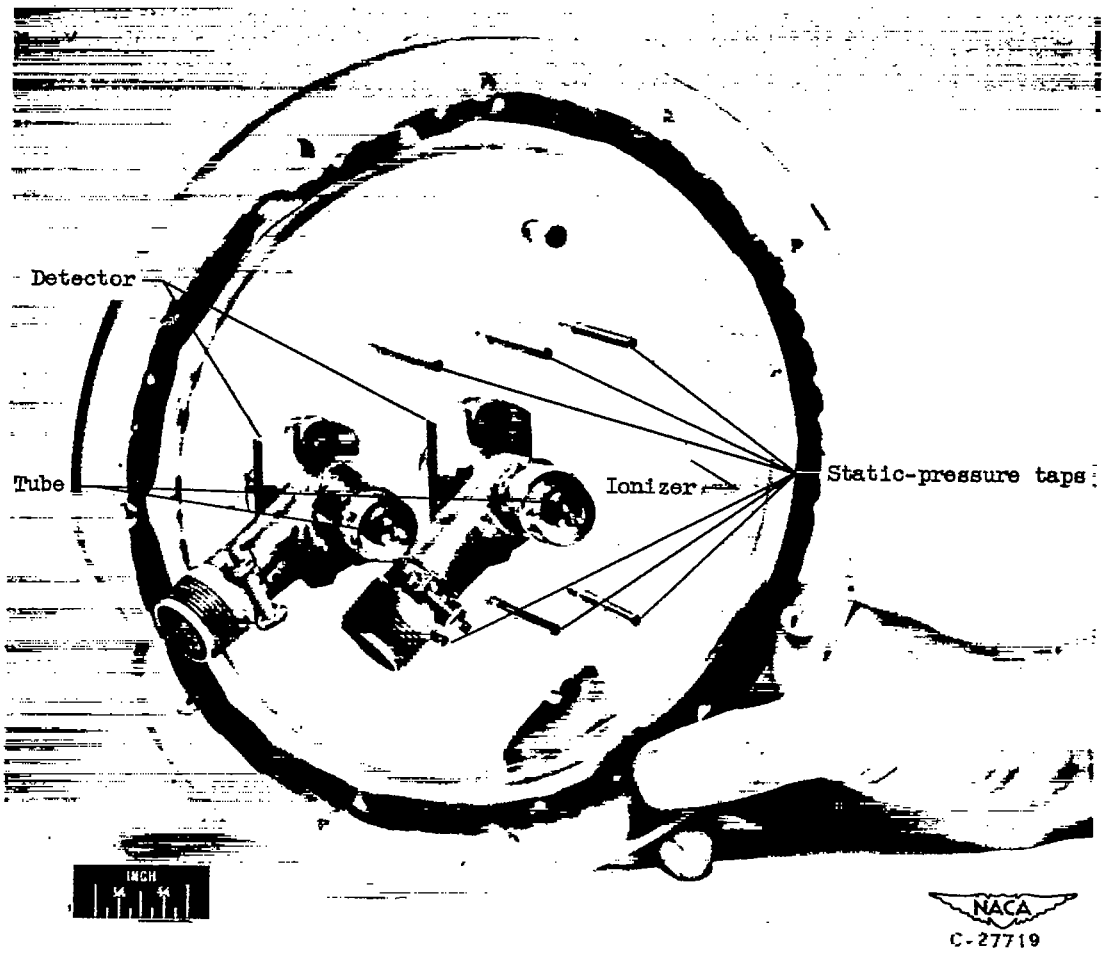

Figure 5. - Wind tunnel wall insert showing ionizer and detectors.

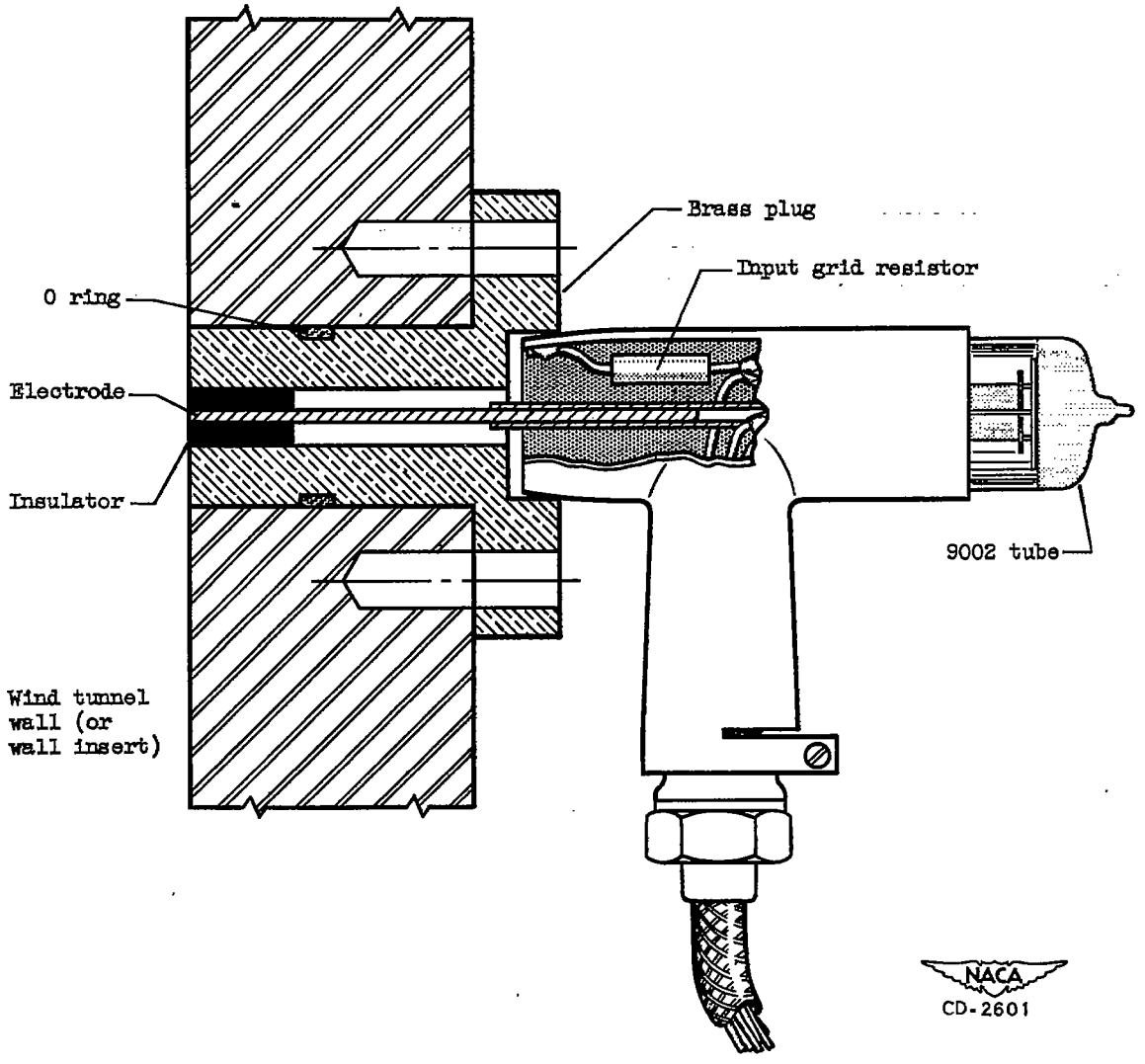

Figure 6. - Detector assembly.

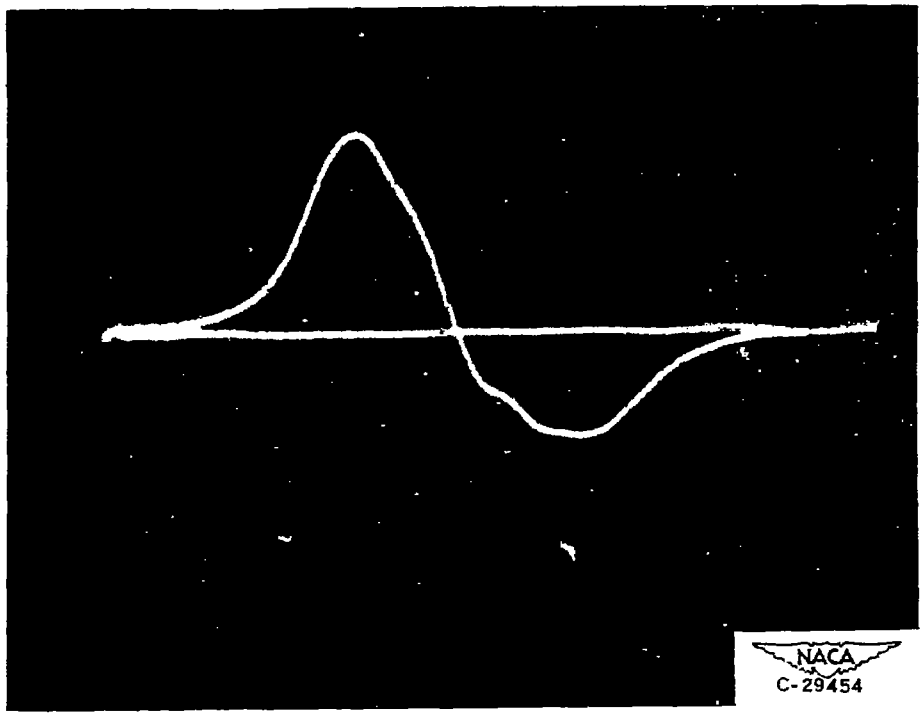

Figure 7. - Typical wave form of voltage pulse induced in detector by passage of ion bundle (ion signal).

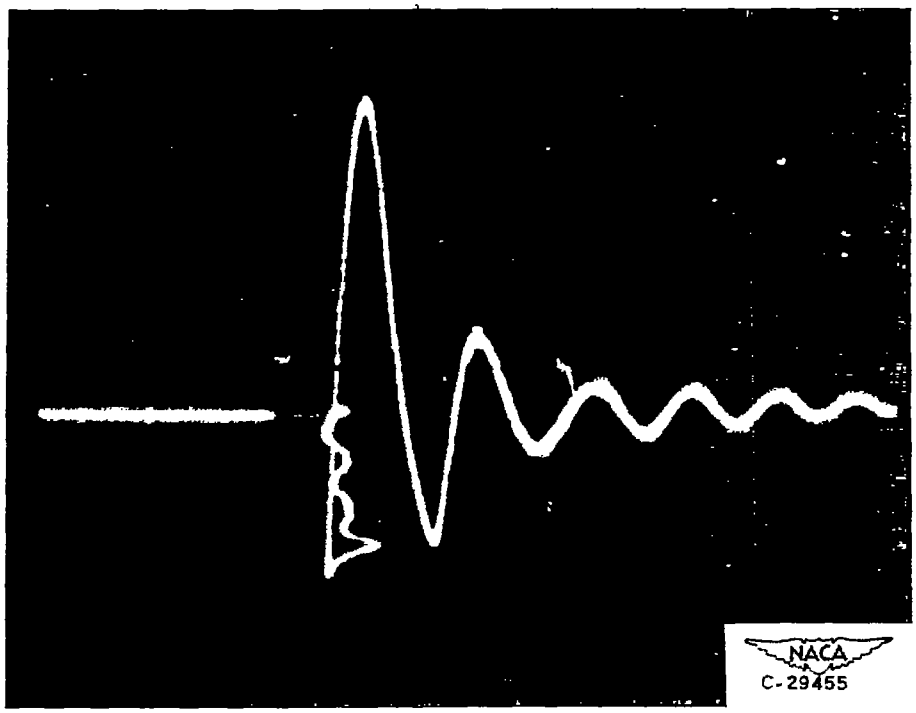

Figure 8. - Wave form of voltage pulse received by direct induction.

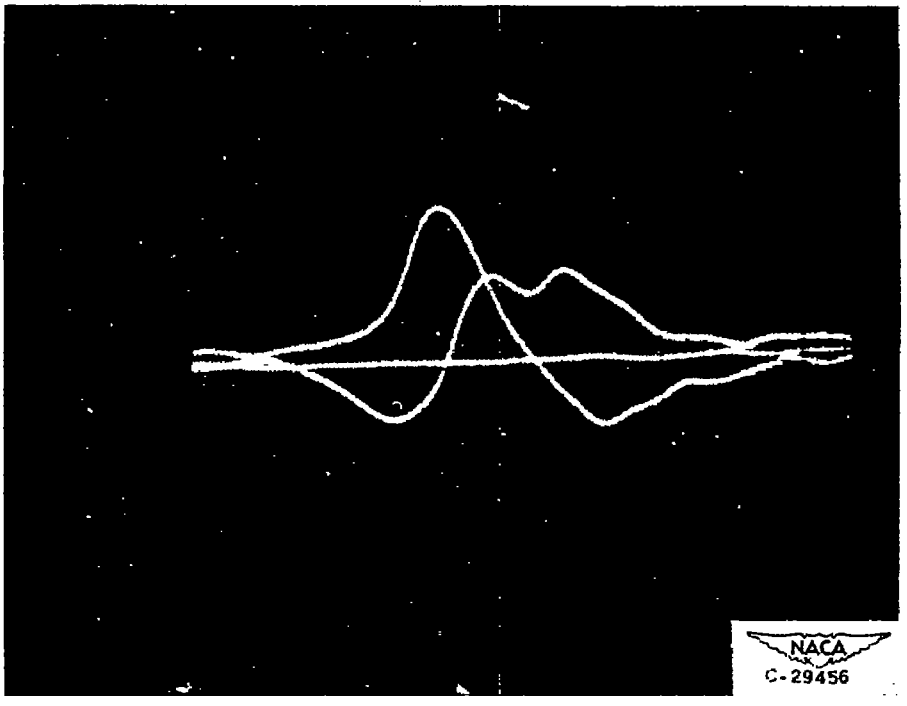

(a) Type II crossover leads that of type I by approximately 90°.

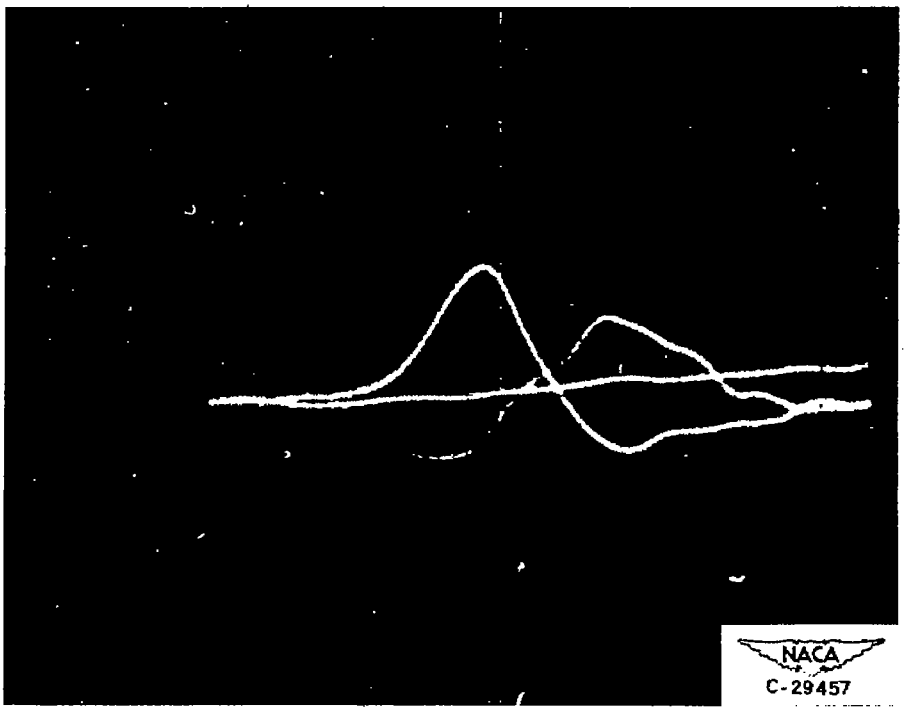

(b) Type II crossover leads that of type I by approximately 45°.

Figure 9. - Wave form of ion signals received by detector. One miss, one type I strike, and one type II strike.

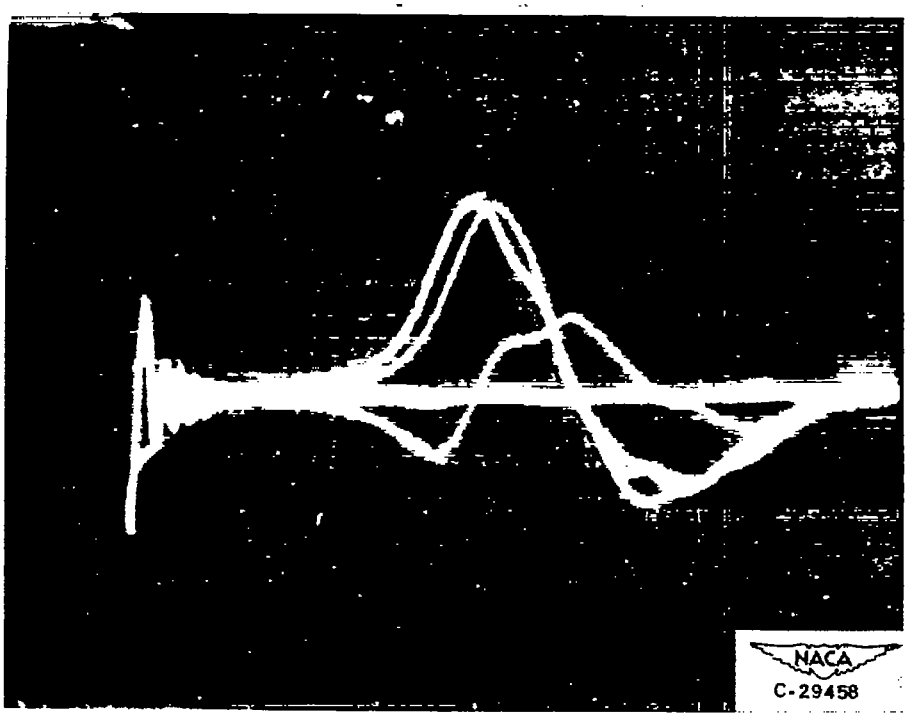

(a) Approximately four misses, three type I strikes, and one type II strike.

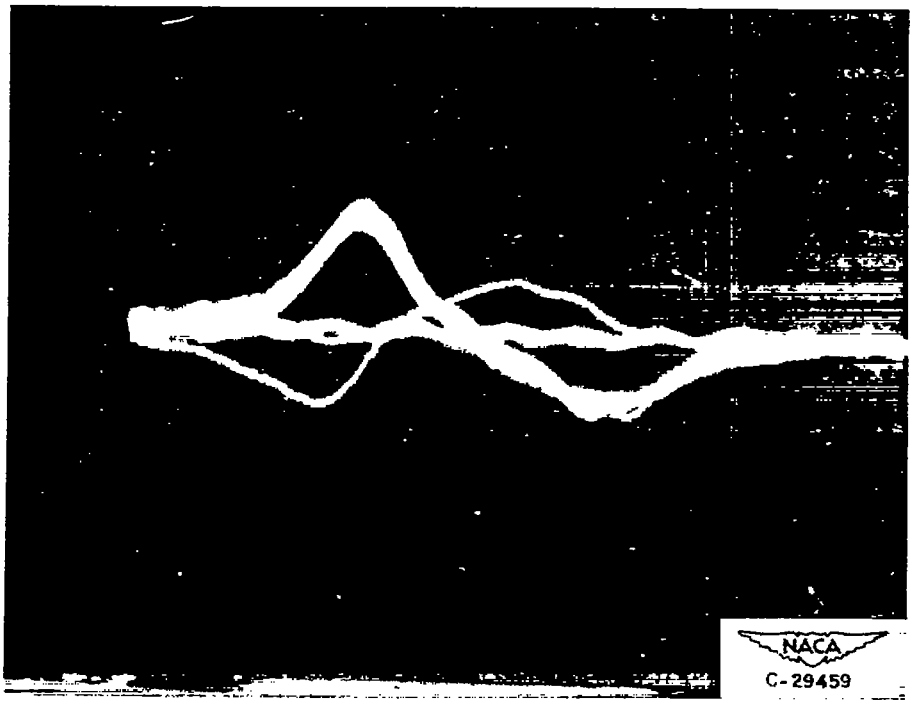

(b) Approximately four misses, five type I strikes, and one type II strike.

Figure 10. - Wave form of received signals.

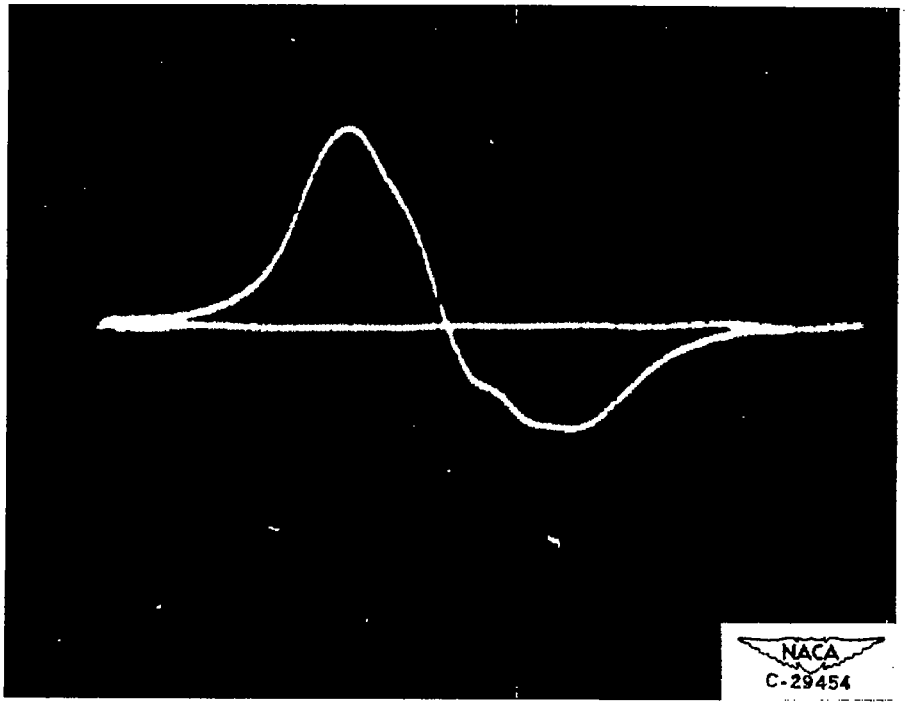

(a) Static pressure, 20.7 inches mercury.

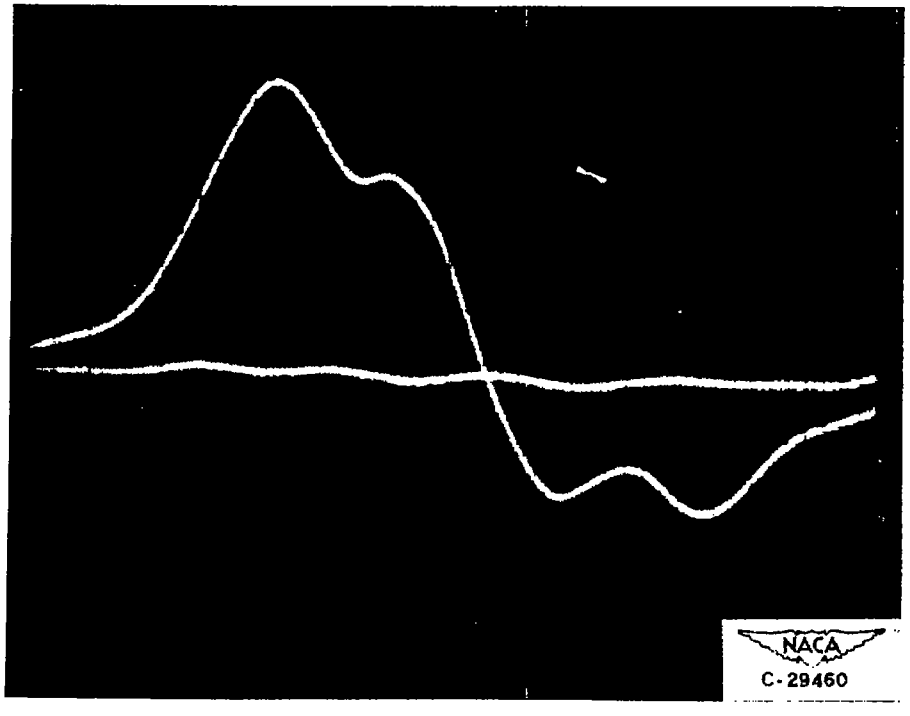

(b) Static pressure, 13.6 inches mercury.

Figure 11. - Wave form of single type I received pulse.

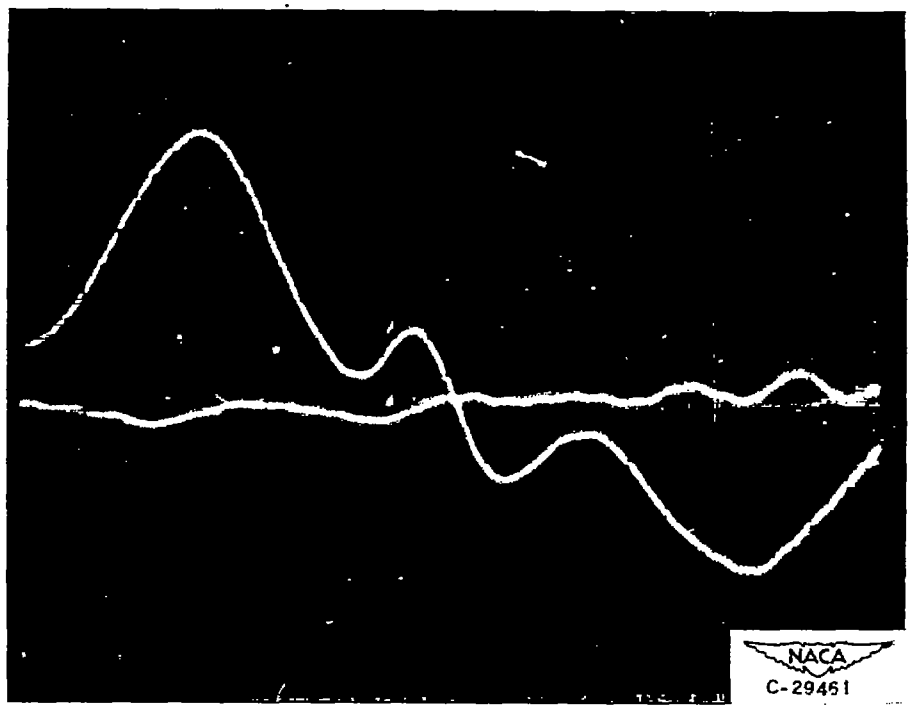

(c) Static pressure, 11.3 inches mercury.

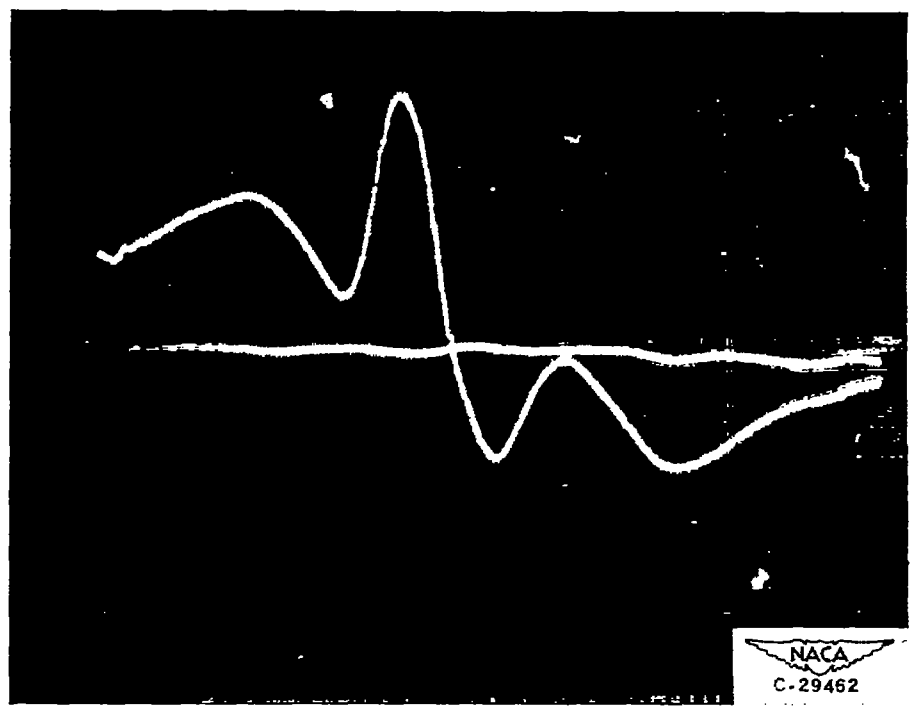

(d) Static pressure, 8.1 inches mercury.

Figure 11. - Concluded. Wave form of single type I received pulse.

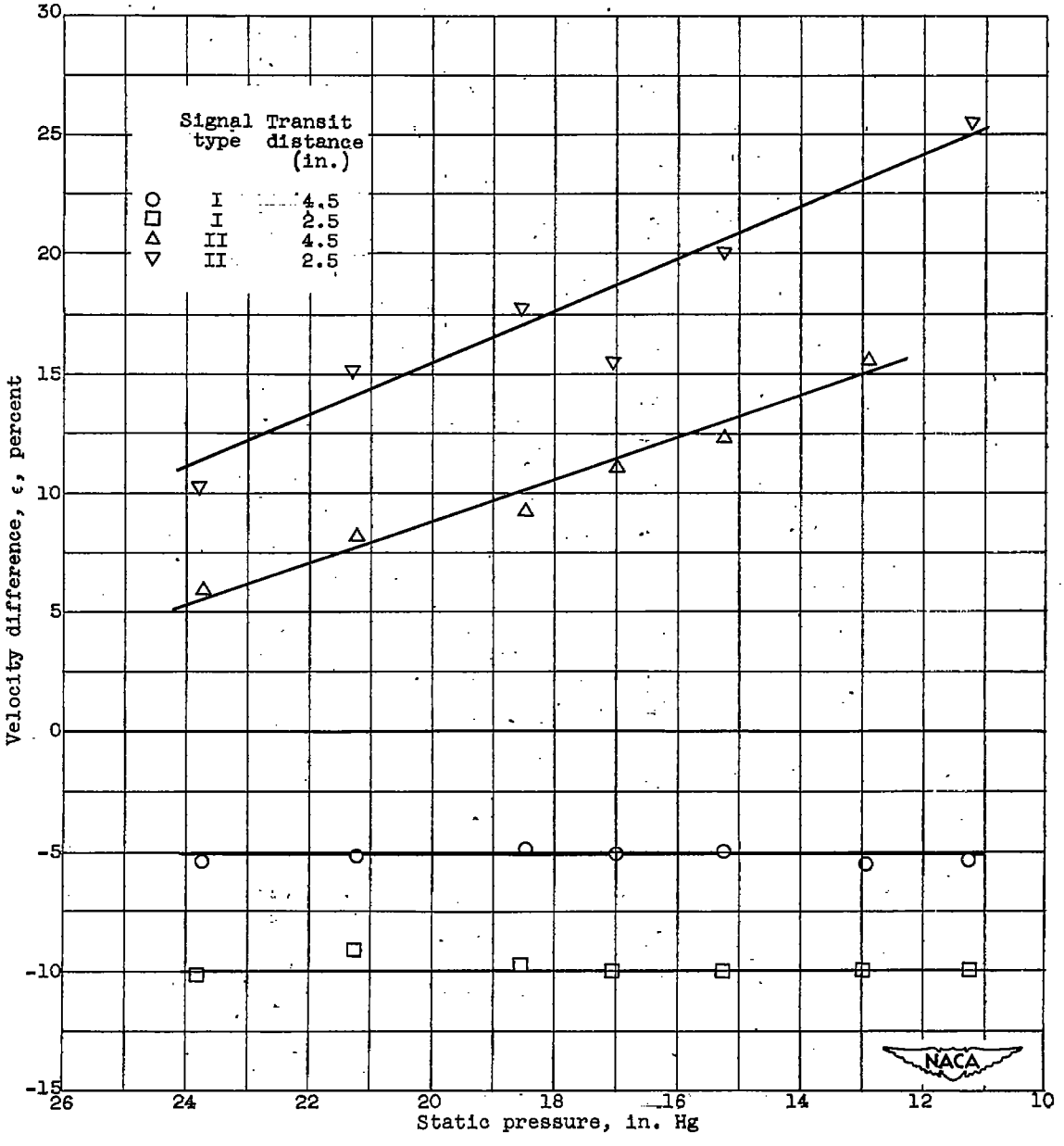

Figure 12. - Comparisons of velocity as function of static pressure using single-detector method at Mach number of 0.7.

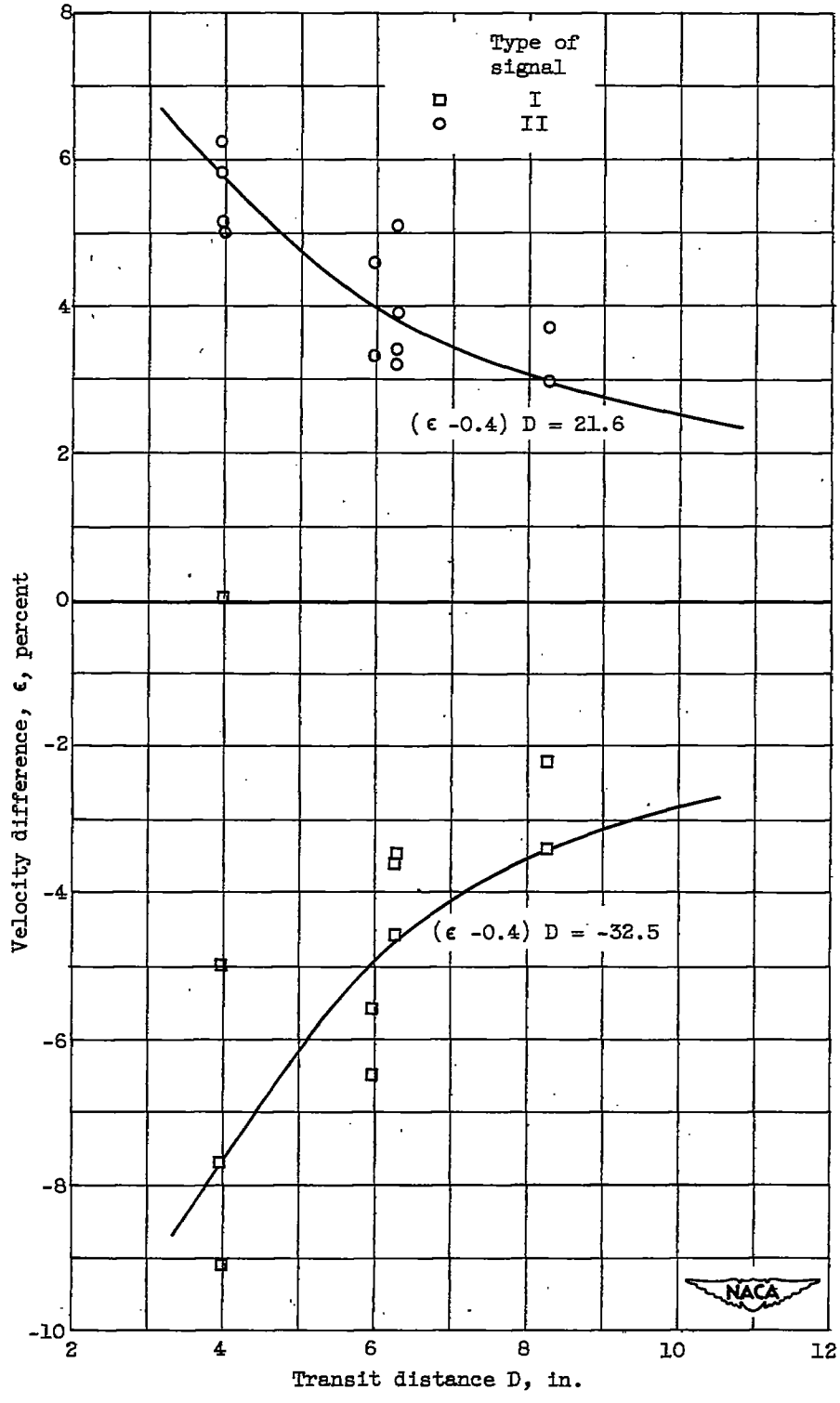

Figure 13. - Comparisons of velocity as function of transit distance using single detector method.

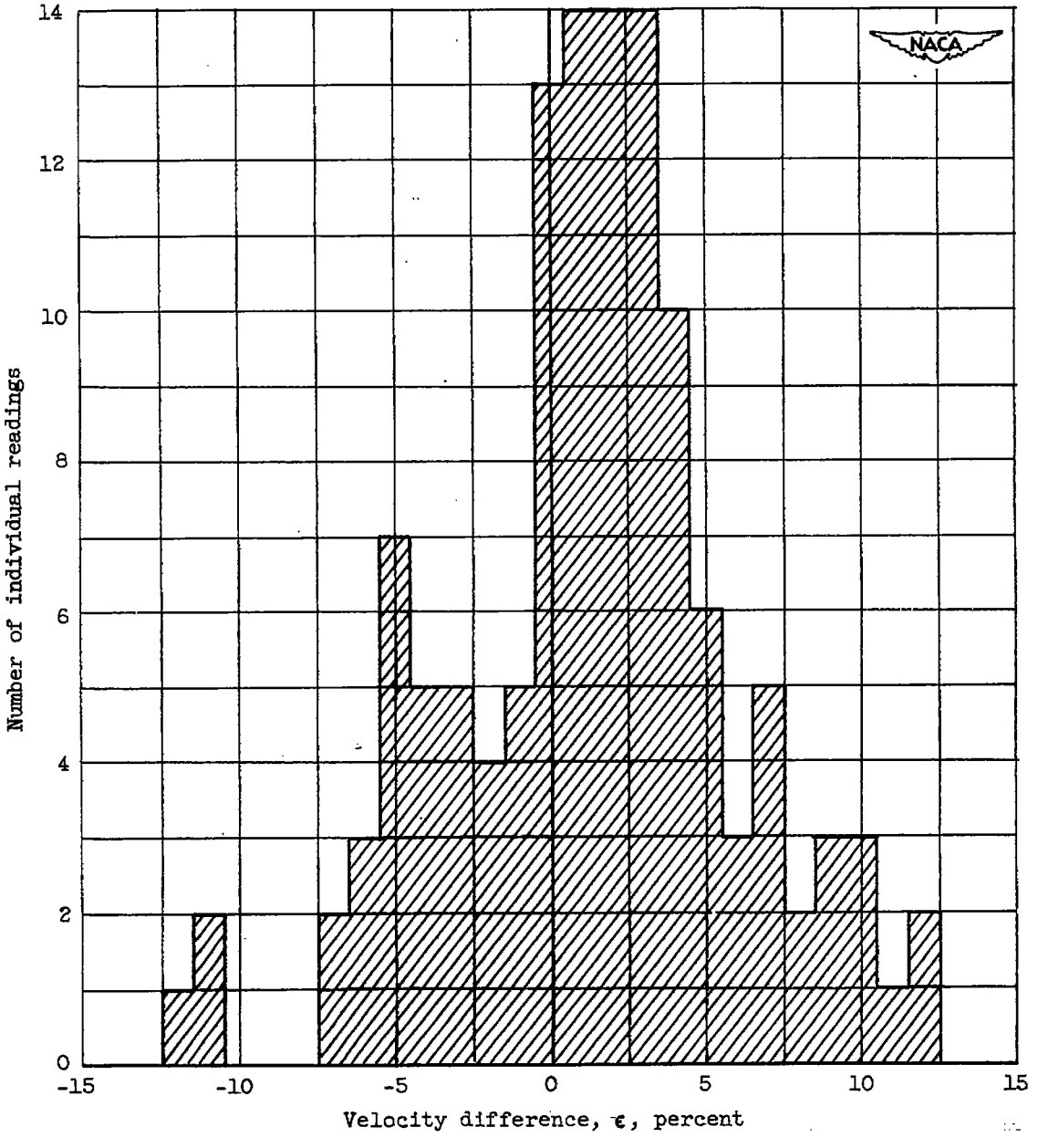

Figure 14. - Distribution of interdetector readings.

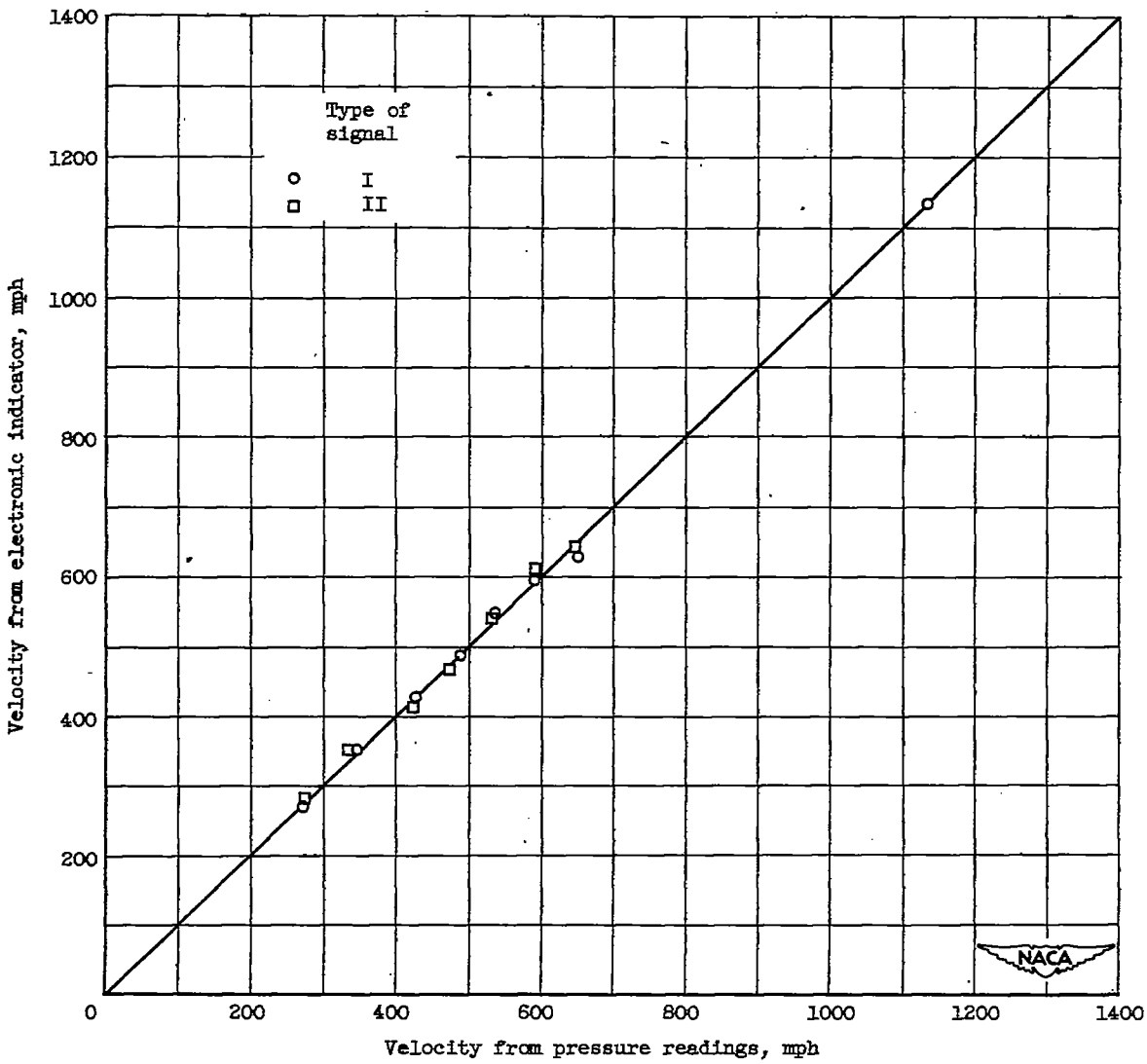

Figure 15. - Comparison of airspeed determinations by interdetector method.

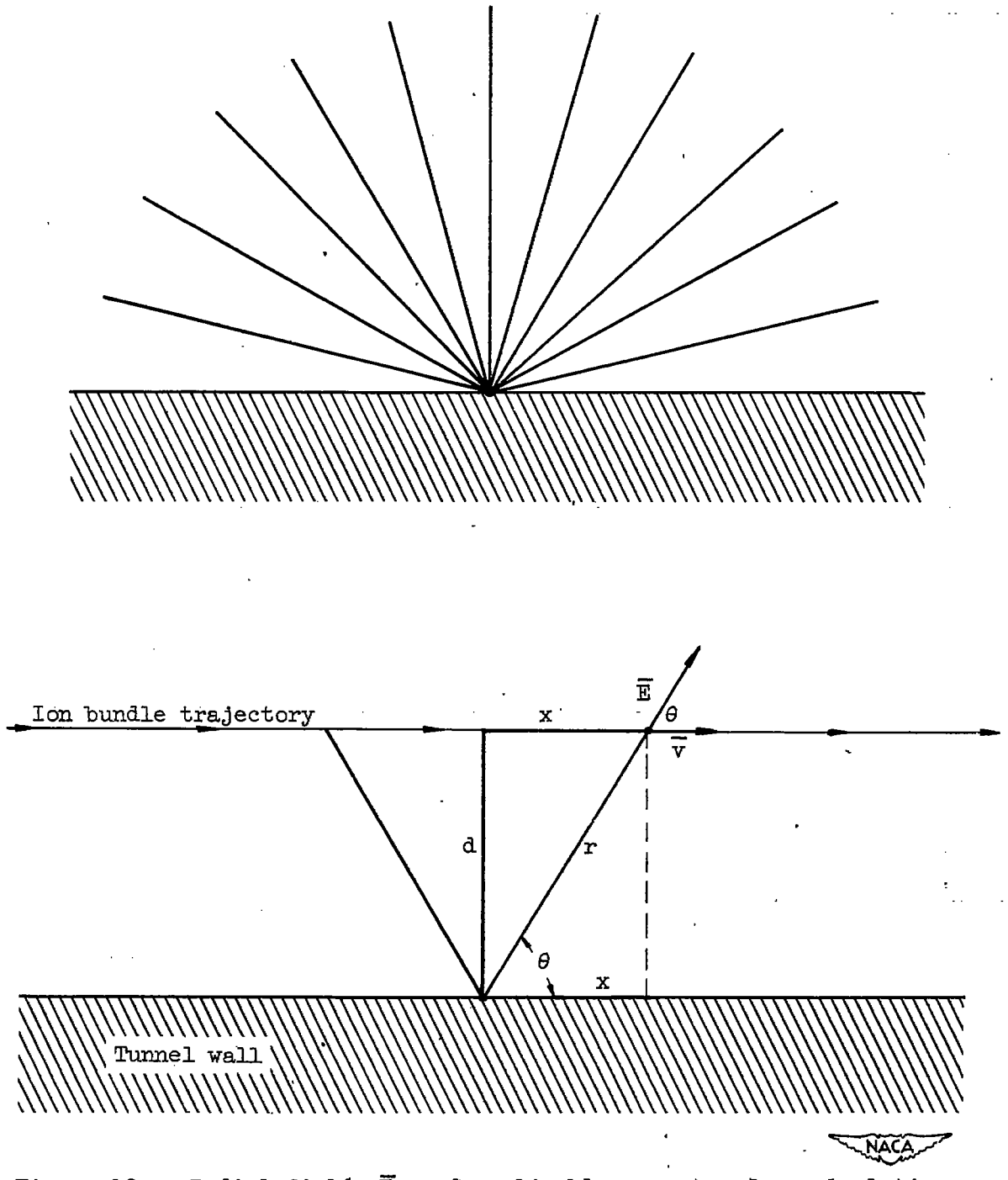

Figure 16. - Radial field $\bar{E}$ and applicable geometry for calculating approach distance d.

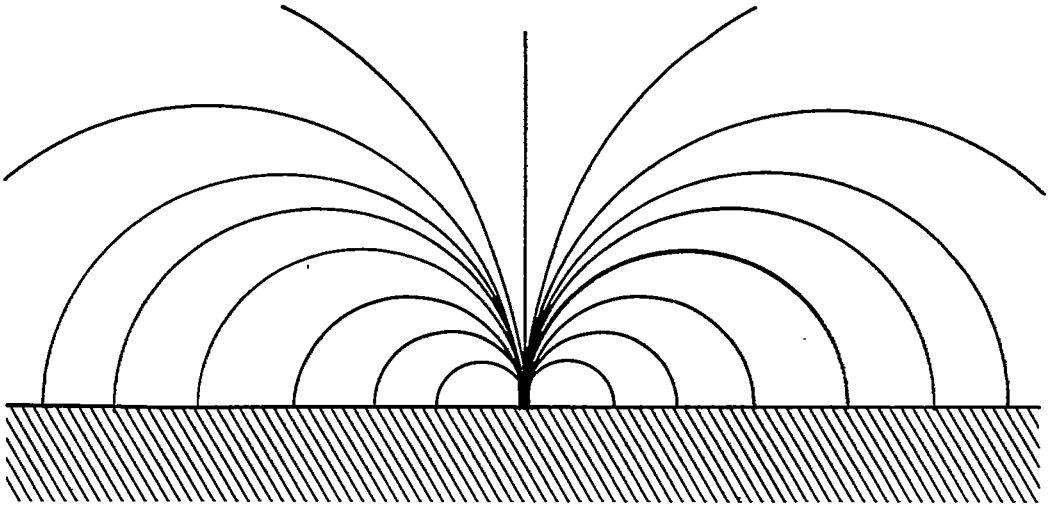

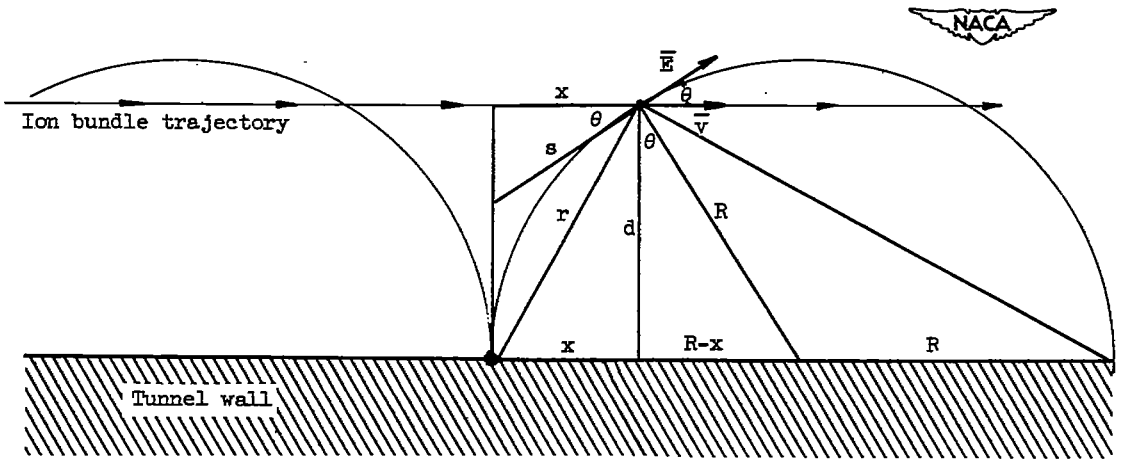

Figure 17. - Circular arc field $\overline{E}$ and applicable geometry for calculating approach distance d.